Timing of aeolian sand transport events on a narrow beach

Z.E.M. van Aartrijk

4083997

Supervisors: P.M. Hage, MSc., prof. dr. B.G. Ruessink

MSc Earth Surface and Water

Department of Physical Geography

Faculty of Geosciences

Utrecht University

June 2018 – January 2019

Utrecht University

Abstract

Modelling aeolian transport in coastal zones is important to understand aeolian transport dynamics and it allows us to secure future stability of dunes as natural coastal defences. Nonetheless, modelled aeolian transport rates based solely on wind-data largely overpredict the actual transport and hence deposition on the foredune. The Coastal Group of Utrecht University has developed a new aeolian transport model, including the most important features suggested by previous studies that limit aeolian transport. These features include wave-runup, storm surges, surface moisture content and more realistic flow patterns of the wind on a beach (local wind conditions). The aim of this study is to evaluate and validate the performance of the model for its compatibility with actual transport events, with a focus on the timing of the model. The intensity of actual transport events was visually quantified with the use of high quality photos taken from the Coast3D tower, located at the beach of Egmond aan Zee. The intensity was quantified based on the size of moving dry patches of sand, the formation of streamers and the formation and movement of sand strips. In total there are five classes defined whereby class 0 indicates no aeolian transport, class 1 indicates a low intensity and the transport intensity gradually increases up to class 4, indicating an extremely high transport intensity. Based on a combination of wind speed and the classified transport intensity, three types of transport are distinguished. The first type of transport event is an unlimited transport event, meaning that the aeolian transport is equal to the wind potential. The second type of transport event is a limited transport event, whereby the transport rate is lower than the wind potential. The last type of transport event is an inhibited transport event, defined as events with no aeolian transport. For each of these transport events, the outcome of the model is evaluated. The model performed correctly for 60% of the time for the unlimited aeolian transport events and limited aeolian transport events. For the other 40% of the events the model generated a zero-transport rate, because the wind speed or wind direction did not exceed the implemented threshold. For the inhibited transport events, the transport rates were strongly reduced which is an important improvement, however even with this strong reduction, the transport rates remain too high to represent actual transport rates. For limited and inhibited events, the moisture content was the most important limiting factor. Nonetheless, the largest improvement for all transport types (unlimited, limited and inhibited) in reducing the overprediction in transport rate, was the result of using local wind conditions. Overall, the timing of the model for generating unlimited, limited and inhibited transport rates has improved greatly compared to the models based only on wind data. Further improvements can be accomplished by re-evaluating the calculations of the minimum width required for maximum transport (critical fetch) and re-evaluating the values for the wind speed and wind speed direction threshold.

Contents

List of Figures

List of Tables

1. Introduction

Aeolian sand transport on beaches plays a key role in the growth of dunes. As dunes protect the hinterland from flooding during severe storms, understanding sand transport and the ability to model aeolian sand transport is essential. Current models are not accurate enough, as concluded in previous studies (Bauer & Davidson-Arnott, 2003; Delgado-Fernandez, 2011; Delgado-Fernandez & Davidson-Arnott, 2011; Sherman et al., 2013; Sherman & Li, 2012). The transport models, based on only the wind speed and grain size, overpredict the transport rate and the transport events. A study conducted by Delgado-Fernadez & Davindson-Arnott (2011) showed that only 1 out of 9 high wind velocities (storms) is associated with a large amount of sediment transport. During the other 8 events, transport was inhibited by transport-limiting factors that can either increase the entrainment threshold or decrease the distance available for aeolian transport (fetch).

The aeolian transport models were based on research conducted in desert environments. The outcomes and equations result in a mismatch when applied to coastal environments, especially narrow beaches (Bauer and Davidson-Arnott et al., 2003). Aeolian transport on the beach is a complex process, in which multiple factors and processes are involved and connected; the narrower a beach, the easier the transport rate is affected. For instance, the wind dynamics and the daily inundation of the beach caused by wave run-up, tidal variation, and occasionally by storm surges, results in a limited fetch zone, especially for narrow beaches. Furthermore, it causes a continuous, moist surface layer (Masselink et al., 2014; Douglas J. Sherman & Li, 2012). As a result of the complex coastal conditions for aeolian transport, models developed in deserts are not applicable for coastal settings, and thus aeolian transport models for beaches need to be constructed.

To improve aeolian transport prediction on narrow beaches, the Utrecht Coastal Group has developed a new model, named Aeolus. This model contains transport-limiting factors such as the spatial and temporal changes in moisture content, the adjustment of wind direction near the dune face, and beach inundation by tides and storm surges. The aim of this new model is to increase the correspondence between model outcome and actual transport events.

The new model needs to be reviewed and analysed thoroughly to ensure accuracy and indicate improvement. This (MSc) research will focus on the evaluation and validation of the outcome for its compatibility with the timing of actual transport events. The aim of this research is to be able to specify under which conditions the incorporated fetch and supply-limitation are most relevant and which of the factors are most important in minimizing the mismatch between Aeolus and actual transport events.

1.1 General approach

As the model needs to work and to be verified on the meso-scale (i.e., seasons to years), obtaining data by field research is too time-consuming to conduct. Therefore, the beach of Egmond aan Zee, the Netherlands, was selected as the study site because of its multi-year video imagery dataset. The beach of Egmond is classified as a narrow beach. The timing of transport events is determined by analysing photos that were taken at one-hour intervals in the years 2013 and 2014. As there is a difference between the start of entrainment and fully developed transport events, the images are classified based on the visible Aeolian activity.

For the same time period, the Aeolus- and the 'wind- only' models calculated the aeolian transport rate. The calculations by Aeolus includes several scenarios with varying settings of the supply and fetch limitations. By comparing the observed aeolian events and their transport intensity classification with the outcome of both models and scenarios, a conclusion can be made if the timing of Aeolus is accurate, or to say in other words, the supply limiting factors switch on at the right moments.

2. Background Literature

2.1 Fundamentals of aeolian sediment entrainment

The entrainment, transport, and deposition of sand particles by wind is an important driver in the creation of geomorphological features like beach and desert dunes. To understand aeolian sediment transport, it is key to understand the fundamental knowledge of entrainment.

The entrainment of the sediment is the result of the relation between wind dynamics and soil characteristics. The wind pattern in vertical direction follows a log-linear shape, see Fig 2.1, whereby the velocity increases with height (Nickling & Neuman, 2009).

The wind directly above the bed entrains the sand particles. The air flows around the soil particles causing a lift force by both the reduction of the static pressure, which acts on top of the grain, and the formation of a steep vertical velocity increase. The lift force combined with the drag force of the wind results in the entrainment of particles under the condition that these wind forces exceed the gravitational and inter-particle forces, such as capillary water tension, soluble salts and cohesive forces (Nickling, 1988). The wind velocity near the surface is called shear velocity (u*) and thus the force generated by the shear velocity needs to exceed the gravitational and inter-particle forces. The shear velocity can be calculated from the wind velocity using the following equation (Keijsers et al., 2014).

1. $$u_z = \frac{u_*}{k} \cdot \ln \frac{z}{z_0}$$

Where u_z is the wind velocity in m/s at the height z above the bed in m, u* is the shear velocity in m/s and k is the Von Kármán constant (≈0.4), and z_0 is the roughness length in m. With equation (1) the shear velocity can be calculated, however, to assess if entrainment will occur, the shear velocity needs to be larger than the critical shear velocity (u_{*t}). The threshold shear velocity can be calculated with the following equation (Bagnold, 1941; Keijsers et al., 2014; Nickling & Neuman, 2009).

2. $$u_{*t} = A \cdot \sqrt{g \cdot d \cdot \left(\frac{\rho_s - \rho}{\rho}\right)}$$

Where A is a dimensionless constant, g is the gravitational accelerations (m/s^2), d is the median grainsize, ρ_s is the density of the sediment in kg/m^3, and ρ is the density of the air in kg/m^3. A typical value for A is 0.1 for a particle characteristic of R_{ep} >3.5 (particle friction Reynolds numbers) (Nickling & Neuman, 2009).

Exceeding the critical shear velocity result in a potential transport event. The first grains that are dislodged are either very small or exposed. The grains first start to shake before entrainment. The actual entrainment might be caused by microscale turbulence in the boundary layer (Nickling & Neuman, 2009). With

increasing velocity and duration of the wind event, more, larger and less exposed grains are entrained. After the initial entrainment of particles, other mechanisms enhances the aeolian sediment transport. These mechanisms will be discussed in the section 2.4.

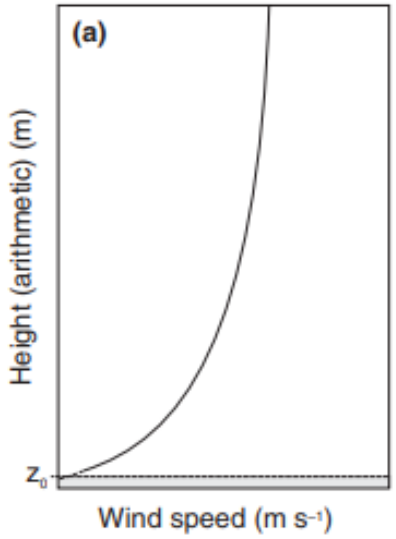

Fig 2.1: Wind speed profile over a surface. Source: Nickling and McKenna Neuman (2009)

2.2 Aeolian transport mechanisms

After entrainment, there are multiple mechanisms that can transport a particle further. The most commonly used classification is that of Bagnold (1941) indicating the following three modes of aeolian transport: suspension, saltation, and creep.

Suspended transport indicates that grains travel large distances or long periods through the air *(Figure 2.1).* A small particle can be airborne for several days and travel thousands of kilometres. The smaller the size of the grain, the longer it can be in suspension. The typical grain size for suspended particles is approximately 70µm, and for long-term suspension, the grains are not larger than 20µm. In coastal environments, this transport mechanism is insignificant as the grains are typically too large to be suspended (Bagnold, 1941; Masselink et al., 2014; Svasek & Terwindt, 1974).

When the duration of the airtime of a particle decreases, the transport mechanisms gradually evolves from suspension into saltation. Saltated transport is a grain which follows a parabolic trajectory for a short amount of time. See Figure 2.2. The magnitude of the trajectory is several decimetres long and a decimetre in height (Svasek & Terwindt, 1974). The exact height can be calculated using the shear velocity and the gravitational force. This type of transport accounts for 95% of the total transport volume on a beach (Masselink et al., 2014; Nickling & Neuman, 2009).

Creep transport is when particles are rolling or sliding over the surface due to the wind (Fig. 2.2). The particles are continuously connected with the bed, indicating that the grains are too heavy to be lifted. Normally this occurs for particles larger than 500µm (Nickling & Neuman, 2009). Even though less than 5% of the grains are transported by creeping, it plays an important role in coastal environments (Masselink et al., 2014), as it is the dominant transport mechanism for dune growth. Due to creeping, sand particles are transported upward of the upwind side of the dune.

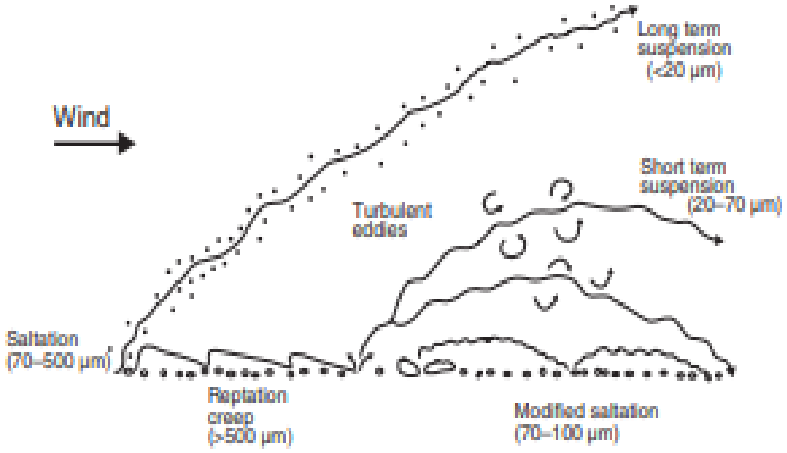

Figure 2.2 shows the different types of aeolian sediment transport mechanisms. Source Nickling and McKenna Neuman (2009)

2.3 Aeolian transport equations

After entrainment, the potential transport rate can be calculated based on the wind velocity. Several equations were proposed based on slightly different experiments. The most commonly known equation was proposed by Bagnold (1941).

3. $$q = C \cdot \left(\frac{d}{D}\right)^{0.5} \cdot \frac{\rho}{g} \cdot u_*^3$$

Where q is the sediment transport rate (kg/ms). However, calculating or determining the shear velocity is complicated. Hsu (1974) proposed an equation containing the shear velocity and provided a factor to relate the shear velocity to the wind velocity. Delgado-Fernandez, and Davidson-Arnott (2011) adapted the equation and incorporated the wind velocity directly into the formula of Hsu (1974):

4. $$q = 1.16 \cdot 10^{-5} \cdot U^3$$

Where U is the mean wind speed in m/s at ~2 m – 10 m above the surface. This equation implies that when the wind velocity increases the sediment transport increases by the power of three. Many of the aeolian transport equations, for instance the equations formulated by Bagnold (1941), Chepil (1945), Kawamura (1951) and Hsu (1971) are based on agricultural land or deserts because of the use of u^3. For each environment, other factors influence the transport mechanisms and supply limitation (Kroon & Hoekstra, 1990). In the following sections, the transport will be specified for the coastal environment and limiting factors will be examined and discussed. Furthermore, the coastal transport models will be evaluated based on theoretical knowledge.

2.4 Fetch and fetch mechanism

The aeolian sediment transport rate over a beach depends not only on the wind velocities as described in the formula of Bagnold and others, but also on so-called fetch effect. Bauer et al., 2009, defined the fetch effect as: '… the progressive increase in sediment transport with downwind distance from a zone of no transport, such as paved surface, leading edge of a sand sheet, or saturated foredune.'.

Fetch effect

The fetch effect can only happen for particles that are saltating. Within the trajectory of a saltating particle, the grains are accelerated by the wind. When a grain hits the surface, its velocity is equal to the wind velocity at the maximum height of the trajectory (Svasek & Terwindt, 1974). Depending on the diameter, velocity and incoming angle of the saltating particle, the impact with the bed can cause re-bounce of the particle. Moreover, the impact can cause ejection of stationary particles. See Figure 2.3. This results in an exponential and asymptotical increase of saltating particles over distance. See Figure 2.4

The available or maximum fetch is the total distance from the upwind to downwind edge. Under ideal condition, the maximum fetch (F_m) is as long or longer than the distance needed to obtain the maximum sand transport rate by the wind, this is called the critical fetch (F_c). At the upwind boundary, the wind has a certain velocity and a certain potential to transport particles. However, there is a lack of transportable material. When the wind 'enters' the beach, sand particles can be transported. Due to the fetch effect, related to the ejection of stationary grains, maximum transport rate is not directly reached at the upwind boundary. The ejection of stationary grains increases over distance and thus there is a minimum length needed to obtain maximum transport.

The length of the critical fetch is variable and is influenced by the wind velocity and supply limiting factors. The critical fetch becomes longer when little sand is available for transport, and thus a longer distance is needed to entrain and transport the same amount of particles compared to a situation with a higher availability of sand. The critical fetch becomes longer as well, when the wind speed is higher. See figure 2.4. This is because the trajectory of the entrainment particles becomes longer for a higher wind speed, and because the transport rate increases with each impact. Thus, if the length increases before an entrained particle crashes back onto the surface then per meter, fewer particles are entrained, and a longer distance is needed to get complete saturation.

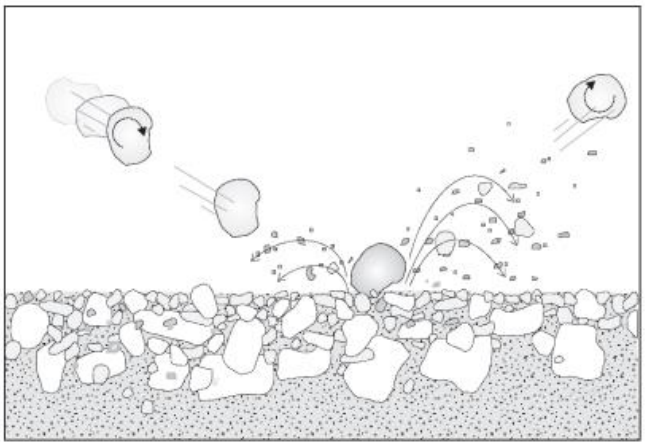

Figure 2.3 schematic image showing the launching effect of a saltating grain crashing into the surface. Source Nickling and McKenna Neumann (2009).

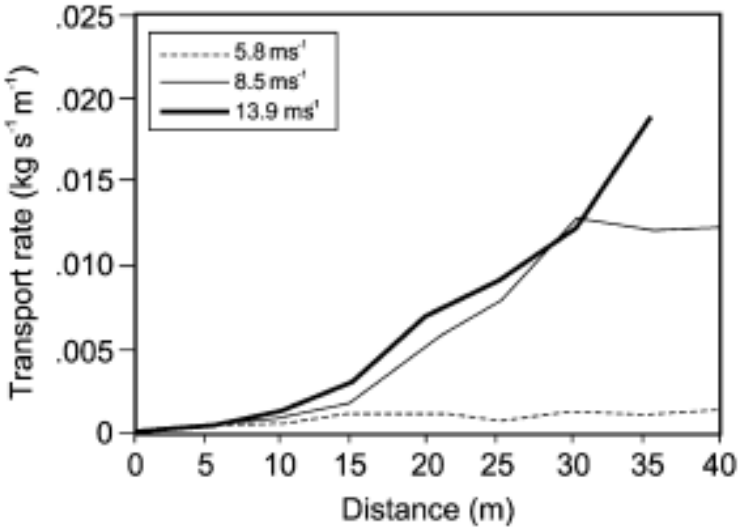

Figure 2.4 the exponential increase of the sediment flux over a distance for different wind speeds. The distance for maximum transport is different depending on the wind speed. Source: Bauer and Davidson-Arnott, 2003

Fetch Mechanism

According to Gillette et al., (1996), there are three main mechanisms determining the length of the fetch effect. These factors are 1) 'Avalanching' mechanism; 2) 'Aerodynamic' feedback; 3) 'Soil Resistance' mechanism. The first two factors cause a lengthening of the fetch effect, while the third factor can either have positive or negative effect depending on the downwind evolution of the soil roughness (Gillette et al., 1996). The 'avalanching' mechanism starts nearly simultaneously with the start of aeolian transport, whilst the other mechanisms establish themselves a certain distance downwind from the location of first entrainment. As described earlier, the impact of the mobilized grains with the soil results in dislodgement of stationary particles (Gillette et al., 1996). From this point onwards, the 'avalanching' mechanism causes the mobile grain concentration to exponential increase.

Avalanching mechanism

The 'avalanching' mechanism was explained by Chepil (1957) as the situation when the impact of a single soil particle sets more than one new sand particle into motion. This results in an exponential increase for a number of saltation lengths until equilibrium is reached. After the entrainment of the first particles by the wind, the transport mechanism becomes self-forcing whereby entrainment can occur at 80% of the critical wind velocity (Masselink et al., 2014). This results in a shift; at initialisation, all particles are entrained by the wind, but this transgressively evolves into a state where all particles are mobilized by the avalanching mechanism (Anderson & Haff, 1988).

Further downwind, the concentration of particles is high, resulting in extraction of momentum from the wind. This extraction reduces the wind velocity, and the particles are accelerated less. With a lower particle velocity, the impact on the bed is reduced and fewer grains are ejected. Eventually, an equilibrium is reached, called 'steady state saltation' (Anderson & Haff, 1988; Delgado-Fernandez, 2010; Nickling & Neuman, 2009). The length over which the self-balancing mechanism develops depends on the amount of ejected grains per impact and the hop-length. As described earlier, the relation between hop-length and wind velocity can increase the critical fetch length. Typical values for the critical fetch length are listed in table 2.1.

Nonetheless, Gillette et al., (1996) found that this mechanism generally results in a fetch effect of a few tens of meters from the edge of the erodible material, indicating that other mechanisms are required to achieve the larger-scale fetch effect. After a few tens of meters either the 'Aerodynamic feedback' or the 'soil resistance' mechanism enhances the fetch effect. Which of these mechanisms is more pronounced depends on the surface roughness.

Table 2.1 shows the relation between the wind velocity and the critical fetch length (third column) measured in several researches. Overshoot is a peak in transport rate followed by a lowering. Source: Delgado-Fernandez (2010)

Publication	Wind speed range ($m\ s^{-1}$)	Fetch distances range (m)	Sediment size (mm)
Davidson-Arnott and Law (1990)	5.9–13.8	10–15 to > 35	0.2–0.33
Shao and Raupach (1992)	8.5–12.5	Length to overshoot = 5 Length to equilibrium >17 Minimum distance for equilibrium = 15	0.2
Dong et al. (2004)	8–22	Negligible to >16	0.18
Spies and McEwan (2000)	7.9–26.9	Length to overshoot = 5 to 30 Length to equilibrium = <20 to >50	0.25

Aerodynamic feedback

The 'aerodynamic' feedback, is also known as the 'Owens' effect, is based on the increase of roughness height caused by the saltating grains (Gillette et al., 1996). The roughness height is determined by the soil roughness. However, Owen (appendix of Gillette et al., 1996) stated that the surrounding saltating grains cause an increase in roughness height as well. The surrounding saltating grains are very dynamic, causing sudden changes in roughness and thus a sudden change in the boundary layer. The planetary boundary layer does not adapt immediately, and thus the effect is firstly confined in the internal boundary layer which expands in the downwind direction. The sudden change in boundary conditions causes a change in the velocity profile of the wind. The near bed wind velocity (shear velocity) increases when the roughness height increases. The increase in velocity causes an increase in the transferring of momentum into the soil, resulting in a positive feedback. As more momentum is transferred into the soil, more grains are mobilized, which in turn increases the roughness height (Gillette et al., 1996; Nickling & Neuman, 2009). The opposite of this effect occurs when the bed becomes smoother, because this reduces the shear velocity and therefore fewer grains are mobilized. Thus, for a rough surface the aerodynamic feedback increases the fetch effect, whereas for a smooth surface the aerodynamic feedback decreases the fetch effect.

'Soil resistance' mechanism

For non-homogeneous sand surfaces, the soil resistance mechanism becomes a more dominant factor in the fetch effect (Gillette et al., 1996). Note that this mechanism can result in positive as well as in negative feedback depending on the downwind evolution of the surface roughness (Bauer et al., 2009). Over time, a rough beach can be smoothened by saltating particles. This effect is known as sandblasting. With the reduction of the roughness of the surface, more of the energy of the wind can be transferred in transporting particles and thus enhances the fetch effect (Delgado-Fernandez, 2010; Gillette et al., 1996). When the roughness increases in downwind direction, more energy is 'absorbed' by the surface and leads to a reduction of transport capacity and result in a reduction of the fetch effect. Note, Bauer and Davidson-Arnott (2003) stated that this mechanism is mostly irrelevant for aeolian transport on beaches.

Sediment transport $F_c > F_m$

When the width of the fetch is longer than the critical fetch, the aeolian sediment transport rate can be calculated by equations 3 or 4. However, on narrow beaches, the actual transport rate is not equal to the maximum transport rate. Bauer and Davidson-Arnott (2003) stated that the increase of aeolian transport is exponential and asymptotic. Delgado-Fernandez (2010) proposed four equations to calculate the transport rate if $F_c > F_m$ and selected the following equation as the most suited equation:

5. $$q_n(F) = q_n \cdot \sin\left[\frac{\pi}{2} \cdot \frac{F}{F_c}\right]$$

In this study, we focus on the situation where the maximum fetch is relatively short. This is often the case on narrow beaches, such as the study site, where the maximum transport is not reached because $F_c > F_m$. Only during highly oblique or alongshore wind events will the maximum fetch exceed the critical fetch.

2.5 Wind dynamics on beaches

The wind characteristics on a beach changes per section; foreshore, mid-beach and back beach. Generally the wind direction changes to a more alongshore direction, as a result of the dunes. The potential of the wind to transport particles reduces in the downwind direction. These changes of the wind start slightly downwind of the water beach interface, where the roughness of the beach surface creates an internal atmospheric boundary layer. Within this boundary layer, the steep velocity gradient results in a large shear velocity creating a large potential sediment transport (Bauer et al., 1990). Even though the potential is high, the actual transport is relatively low. The results of Bauer et al., (2009) showed that the highest transport rate was mainly measured in the mid-beach section. At the upwind boundary, particles are only entrained by the wind, and so the transport rate is low, despite the high potential (Bauer et al., 1990). In downwind direction, the internal boundary layer expands, reducing the steepness of the gradient and likewise reducing the shear velocity. Despite this reduction, the absolute transport in the mid-beach section is larger than at the shoreline due to the fetch mechanisms described in the previous paragraph. Near the dune foot, the transport rate reduces (Bauer et al., 2009), which can have different causes. Firstly, it can be caused by further vertical expansion of the internal boundary layer and therefore a reduction in wind velocity and likewise a reduction in the transport rate. Another explanation for the reduction is sheltering by, for instance, vegetation or by morphological features, such as embryo dunes (Davidson-Arnott et al., 2008).

The strongest wind rarely result in large transport rates because these events are accompanied by strong storm surges and rain (Delgado-Fernandez & Davidson-Arnott, 2011a). High wind events can even result in dune erosion when the whole beach is inundated by a storm surge and waves crash into the dune face. The results of Delgado-Fernandez & Davidson-Arnott (2011) indicated that low to intermediate wind events are the main conditions for which sediment is transported.

Oblique winds

Depending on the width of a beach, the incoming angle of the wind can influence sediment transport greatly. On wide beaches, regardless of the incoming wind angle, the critical fetch is smaller than the available fetch length and thus maximum transport is (almost) always achieved. For (narrow) beaches, a shore-normal wind direction results in the smallest fetch length possible. For alongshore wind directions, the length is not limited by either the dune row or the water interface. Therefore, the fetch length becomes infinitely long, the critical fetch is exceeded, and thus transport is at a maximum. The higher the incoming angle for the wind is compared to shore normal, the longer the fetch and the higher the potential transport become. Nordstrom and Jackson (1993) indicated that during oblique wind, more sand was transported than during stronger wind events with a shore-normal wind approach. Therefore, the incoming angle of the wind is an important factor for determining the transport rate.

2.6 Moisture content

Aeolian sediment transport rate on beaches is influenced by water in the surface layer. (Bauer et al., 2009; Davidson-Arnott et al., 2008; Walker et al., 2017). Starting at the basis, dislodging of stationary grains is likely to be affected by the moisture content. The fluid stress in the soil increases the initial threshold for lifting by the kinetic wind energy. Furthermore, the moisture reduces the number of particles ejected by the impact of rain (R. G. Davidson-Arnott et al., 2005). The moisture content on the beach differs for the different sections (foreshore, mid-beach, and upper-beach). Commonly, the moisture content of the surface decreases from the foreshore to the back-beach as a result of the regular inundation of the foreshore due to the tide and wave run-up. The greatest transport rates are during low and rising tide because the surface is relatively dry and therefore the capillary force is relatively weak (Nordstrom & Jackson, 1993). Besides the tide, other factors such as precipitation, groundwater table, air humidity and inundation by storm surges, can cause an increase in surface moisture content (Davidson-Arnott, 2006).

A high moisture content decreases the aeolian sediment transport as a result of a higher particle entrainment threshold. With a medium moisture content between 4-6% a higher wind speed is required to initiate sediment transport (Davidson-Arnott et al., 2008). In other words a medium moisture content causes a significant reduction in entrainment and (potential) sediment transport compared to dry conditions (Bauer et al., 2009; Davidson-Arnott et al., 2008; Delgado-Fernandez, 2011; Nield & Wiggs, 2011). Delgado-Fernandez (2011) indicated that with a moisture content above 10%, no aeolian sediment transport could occur, regardless of the wind velocity.

The moisture content reduces the transport directly and indirectly. The direct consequence of high moisture content, is as aforementioned, an increase in the entrainment threshold because the fluid in between the grains binds the grains together by cohesive and adhesive forces (Nickling & Neuman, 2009; Wiggs et al., 2004). The indirect consequence of high moisture content is diminishing of the 'avalanching' effect. For each saltating grain impact, fewer grains are ejected into the air compared to an impact on dry soil (Davidson-Arnott et al., 2008). The exponential growth of saltating particles is reduced, and a longer fetch distance is needed to achieve maximum transport (Davidson-Arnott et al., 2005; Davidson-Arnott et al., 2008). However, this indirect effect is more complex because, despite the reduction in dislodging grains, the sand in combination with water results in a hard-packed surface. The hardness of the surface enhances the avalanching process and the saltation height (Nield & Wiggs, 2011). The saltating particle loses less energy when colliding with a hard wet surface in contrast with a dry loose surface. Nield & Wiggs (2011) concluded that both the moisture content as the hardness of the soil influences the sediment transport. The complexity of which of the two factors is more dominant determines on the drying on the surface and the related adhesion structures that develop due to spatial moisture content differences (Nield et al., 2011).

The results of Davidson-Arnott et al. (2005 and 2008) showed that sediment transport in the upwind area is greatly influenced by the moisture content while in the downwind area is influenced significantly less. Several processes cause this difference in influence. First of all, the entrainment of particles in the upwind area is by wind. In the downwind area most of the grains are mobilized due to the 'avalanching' effect or

'aerodynamic roughness' mechanism (Gillette et al., 1996). As described above, the moisture content influences the initial entrainment by wind more than the avalanching effect. Furthermore, the saltating particles from upwind accumulate in the downwind area. Most likely, the large amount of deposited grains reduces the surface moisture content (Walker et al., 2017). Reducing the wetness of the sediment result in a similar decrease in the entrainment threshold (Bauer et al., 2009). The moisture content of the back beach is not per definition lower compared to the upper beach. The moisture content in the back dune can be higher due to sheltering by foredunes and vegetation (Davidson-Arnott et al., 2008). In the upwind area, the wind erodes the dry surface layer exposing the underlying damp layer. Therefore the new sediment layer needs to dry before it can be eroded leading to a drying-erosion cycle (Nield et al., 2011). To conclude, a higher transport rate can be achieved in the downwind part because the surface moisture content is less pronounced and the accumulation of grains transported from the upwind area reduces the moisture content.

2.7 Aeolian transport Models

As mentioned before, Aeolian sand transport on beaches is of great importance for the growth and stability of dunes and thus coastal protection. In order to access the future safely, transport models are developed to predict the evolution on meso-time scales (years).

In the last century, a number of models was developed by, among others, Bagnold (1937), Kawamura (1951), Zingg (1953), Owen (1964), Kadib (1965) and Hsu (1971). The models were all based solely on the relationship between wind velocity and sediment transport ('wind-only' models) as observed in desert environments. Sherman and Li (2012) re-evaluated these models by comparing them to field data. The results showed that all of the predicted transport rates exceeded the observed transport. The authors suggested that the best model 'ceteris paribus' should be supplemented with a surface moisture correction, although the improvement by this feature can be argued. In another experiment, Sherman et al. (2013) compared the models with nearly ideal field data, where, for example, the moisture content must be below 2%. Regardless, the models still predicted higher transport rates than observed. In both researches, Sherman and Li considered to calibrate the models to the local conditions. For the second research the models were indeed calibrated and the quality of the predictions improved. Despite this improvement, the concept of a model is the universal usage of the models and calibrating the model for each location undermines this concept. Therefore, calibration was not suggested as a solution for the overprediction.

In 2003 Bauer and Davidson-Arnott wrote an article with the purpose to provide a framework for modelling Aeolian sediment transport into the dune system. This framework was general in the sense that the framework did not allow quantitative predictions and that it remained conceptual. Within this framework, the wind direction, beach geometry and fetch effects were incorporated.

Delgado-Fernandez (2011) developed a model including both the framework formulated by Bauer and Davidson-Arnott (2003) and the suggested incorporation of surface moisture content by Sherman and Li (2012). The influence of the surface moisture content was taken into account. However, the model required a surface moisture content map as input data, requiring a field study before the model was usable. Delgado-Fernandez (2011) determined the moisture content on the pixel brightness of the images taken by the present camera system.

The model consists of two main components. First, the filtering of the data based on the following criteria: wind speed (u >6m/s), wind direction (onshore component), surface moisture content (μ<10%) and beach coverage by either snow and ice (<50%) or inundation by nearshore processes (width is 0m). The second component is the classification of the potential transport period based on the controlling variables. After the classification, the model uses the assigned formula. Delgado-Fernandez defined three main classes:

1) Dry condition – no restriction (i.e. potential transport);
   6. $q_n = 1.16 \cdot 10^{-5} \cdot U^3 \cos\alpha$

   Where α is the angle of the wind whereby cross-shore is 0°.

2) Dry condition – restriction which can be divided into restriction as a result of wind speed, the formula excludes F. Or as a result of wind direction, formula includes F. The fetch (F) is the distance between the mean values of the shoreline position (upwind boundary) and the vegetation (downwind boundary);
   7. $q_n = q_n \cdot \sin\left(\frac{\pi}{2} \cdot \frac{F}{F_c}\right)$
3) The last class is moist conditions which can be divided into uniform and spatially complex moisture conditions. As there is no specific equation formulated for the transport on a wet surface, Delgado-Fernandez increased F_c with 50% when the moisture content is between 4%<μ<6% and with 75% for 6%<μ<10%. In situations where μ>10% there is no transport and for the situation whereby 2% < μ < 4% the critical fetch was not adjusted.

The formulas for the limited scenarios are simplified as the focus of this study was to analyse the consequences of incorporating the two components rather than selecting the most suitable equations.

The model simulated the aeolian transport rate for the beach at Greenwich Dunes, Prince Edward Island (PEI) National Park, Canada. This beach is narrow (width 30-40 m) and microtidal. The results indicated that the additional features indeed reduced the transport rate. With only filtering on wind speed and direction, the cumulative transport was 86.458 kg/m which was about 29 times higher than the measured deposition of 3017 kg/m. When incorporating all the features the transport rate was reduced to a total of 18.663 kg/m. Even though this is still 6.2 higher than measured, the outcome of the model is improved.

In addition to the 'wind-only' models more parameters, for example, the fetch or average moisture content, are included to decrease the predicted transport rate (Delgado-Fernandez, 2011; Delgado-Fernandez & Davidson-Arnott, 2011). These parameters are refining the predictions and instead of a prediction of an order of magnitude too high, the predictions are now in the same magnitude. The

difference in transport rate occurs because the transport periods in models are longer than the actual transport events. Another reason is that the strongest wind events and short periods of medium breezes (6-8 m/s) generate no or significantly less transport than the models.

Suggested improvements are to incorporate spatial and temporal variation in wind dynamics (Barchyn et al., 2014) and supply limiting factors (de Vries et al., 2012; Delgado-Fernandez, 2011). Especially supply limiting factors as moisture content and variability in the shoreline (Bauer et al., 2009) will improve the performance of the models. The advantage of creating a spatial and temporal variability is the ability to indicate locally what level the threshold and critical fetch distances should be and which is more representative for the actual conditions (Masselink et al., 2014; Nickling & Neuman, 2009).

To conclude the whole process for entraining particles up to aeolian transport on meso-scale consists of complex mechanisms affecting each other. Formulating and designing a model that incorporates this complexity systematically and accurately has been a challenge. New models, for example, the model created by Delgado-Fernandez (2011) has improved the model outcome from 29 times to 6.2 times the measured transport rate. Further development, therefore, needed to develop a model which corresponds fully with the natural situation in both the quantity of the transport rate as well as the timing of these transport events. Based on the of the previous studies the Coastal Group of the University of Utrecht has developed a new model results which incorporates more supply- and fetch limitations. The details of the new model are explained in section 3.4. This MSc research will evaluate and validate the outcome of the newly designed aeolian sand-transport model, named Aeolus, for its compatibility with actual transport events, with a focus on the timing of the events. The evaluation and validation will be executed in such a manner that the following research questions can be answered:

Is the timing of aeolian transport events improved by incorporating fetch and supply-limitation?

This research question can be divided into two sub-questions:

Under which conditions are the fetch and supply-limitation most relevant?

Which of the fetch or supply-limiting factors is most important on a timescale of years to minimize mismatch between wind-only and actual transport events?

By answering these questions, a constructive analyse can be made, and an indication can be given if further development is needed and if so for which condition or/and factor needs adaptation.

3. Methods

3.1 Study site

The study site lies at the Central Dutch coast, just south of the town of Egmond aan Zee, the Netherlands (Fig. 3.1). The beach width ranges between 30 and 100 meter depending on the semidiurnal tidal elevation. The tidal elevation fluctuates between 1.4 m during neap tide and 1.8 m during spring tide. The tidal pattern is asymmetric where the high-water crest of the tidal waveannu travels faster than the low water trough. The average offshore wave height and period are 1.2m and 5 seconds, respectively. During storm conditions, the wave height can be up to 5m and for Northwesterly storms. Storm surges can be more than 1 m which can flood the gently inclined (1:30 m) beach for several days (Hage et al., 2018a) The intertidal beach often includes two slipface bars. The dominant wind direction is south to southwest and combined with the north orientation of the beach (7° declination to the east) results in a strong oblique wind climate. The sand on the beach has a grainsize of 240 µm. The downwind boundary of the beach is the foredunes, which form a continuous parallel lineation with a height of 20-25m (Hage et al., 2018). The foredunes exhibit a steep seaward front caused by occasional erosion events. The foredunes are densely vegetated with European marram grass (*Ammophila arenaria*).

Figure 3.1 Location of the field site and weather station: source (Hage et al., 2018b)

3.2 Input data

Weather and water data were provided by the Royal Netherlands Meteorological Institute (KNMI and Rijkswaterstaat respectively). Water measurements are taken at Stroompaal IJmuiden. The wave height, swell height, water levels, and storm surge were measured every 10 minutes. Wind data was measured at KNMI station IJmuiden which is located approximately 20 km from the study site. The wind data was obtained from two data sets. The first data set is openly accessible and contains the wind direction and the wind speed for each hour. There are three types of wind speed: highest wind gust, the hourly mean

and the wind speed that is the average of only the last 10 minutes of the hour. The second data set was obtained on request and contains the same information, although the accuracy was much higher. In the first data set, the wind direction measurements are rounded to 10^{o} and the wind velocities to 1 m/s, while for the second data set the precision is 0.1^{o} and 0.001 m/s, respectively. The first data set was used to select the images and the second data set was used for the model. The wind data of the second data set is visualized as a wind rose (Fig. 3.2). The dominant wind direction in the years 2013 and 2014 was southwest and this direction also includes the strongest wind events. This dominant southwest wind direction results in a strongly oblique character and thus matches the general conditions described in the study site paragraph.

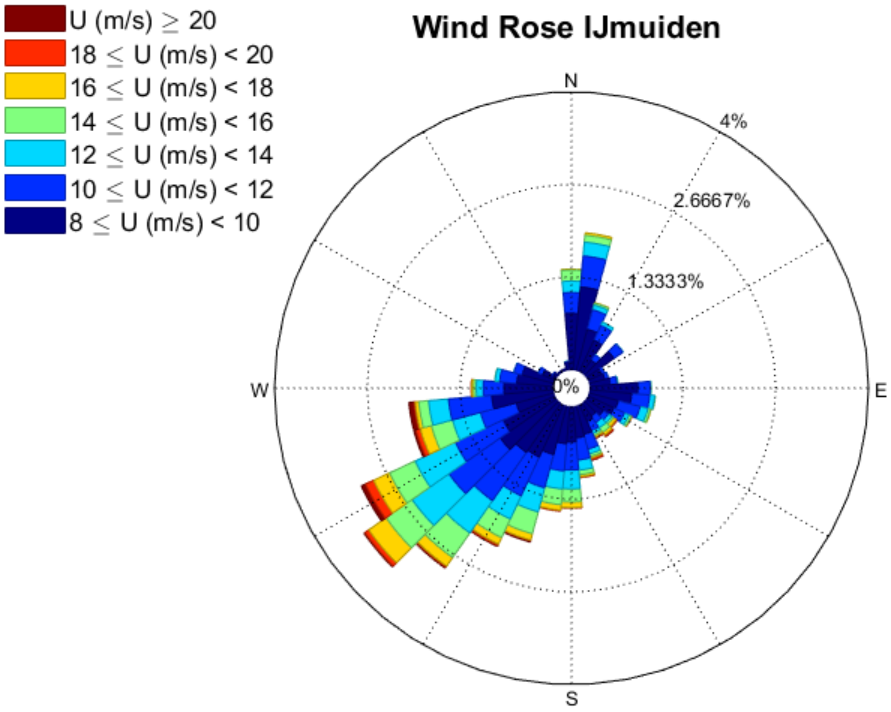

Figure 3.2 shows the wind direction, the frequency and the velocity of the wind in 2013 and 2014 measured at IJmuiden.

3.3 Argus imagery

At the beach of Egmond, five RGB-colour cameras are attached to a 45 m high tower, which have been monitoring the beach from 1998 to 2015. This Argus video system generates a snapshot, a time-exposure, and a variance image. The images are taken every 30 minutes and are usable when taken with sufficient daylight. Multiple oblique images are taken which can be merged together for a 2D plan view of the beach. The image used for this research has a resolution of 1392 x 1040 (Hage, 2014). The pixels cross-shore side is constant and represents about 0.2 m of the beach. The alongshore footprint dimension of the pixel increases with distance from the tower. At 100 m from the tower the dimension of the pixel is 0.2m and increases to a dimension of ≈1.5m at a distance of 400 m (Hage et al., 2018).

The images from 2013 to 2015 were analysed to indicate the Aeolian transport intensity. First, a selection based on the wind speed on the exact moment the photo was captured. The critical wind velocity for sediment entrainment is 8 m/s. This value not determined by measurements, but based on Argus images (Hage et al., 2018b). For each hour in daylight that the wind speed matched the criterion, two images were selected. The reason for analysing two images per time step is to do a more reliable analysis, as well as that in the situation that the image of one of the cameras was unclear, the other image could be analysed. The 2D overview images were formed by combining the images of all the cameras, and the photos taken by the southward looking camera 5. As the overview images show the north and south part of the beach, the images are useful for the overall transport intensity for the whole beach. However, to analyse the images in more detail, the images from camera 5 were analysed. The selection for the images from camera 5 was wider in order to have an additional check if indeed no transport occurs below the threshold of 8 m/s. For each day whereby the criteria were matched, all of the images from that day were selected and analysed. In some circumstances, no class is applicable due to poor vision, caused, for example, by raindrops, ice on the camera lens, or thick fog.

The transport intensity is classified by using the movement of dry patches of sand, spatial variation in streamers and the formation of bedforms. Observing any of these features often requires the contrast between dark wet sand and light dry sand (Hage et al., 2018; Bauer and Davidsonn-Arnot 2002; Nield et al., 2011; Nield 2011). There are 5 classes in total (see Fig. 3.3).:

Class 0	there is no visible sign of aeolian transport.
Class 1	low intensity transport. Small patches of dry sand are moving slowly over the beach.
Class 2	medium intensity transport. Large patches of dry sand are moving over the beach
Class 3	high intensity transport. Signs of aeolian streamers and the formation of sand strips of a beach full of sand strips who are barely moving.
Class 4	extremely-high intensity transport. The beach is covered with moving sand strips or a high intensity of streamers.

To determine under which conditions the model performs best, the classified transport events are divided into different categories based on the wind velocity (Table 3.1). The wind classification is determined by Hage et al., 2018b, and is mainly based on the wind velocity and to some degree to the potential transport. The model results will be divided using the same wind classification, which facilitates comparison for the Argus and model results. Note that the wind velocity is listed for both the regional and local conditions. As mentioned in chapter XXX, the wind characteristics change over the length of a beach. The model can use both the regional and local conditions, and therefore, the wind speed thresholds are listed for both the regional and local conditions.

Table 3.1 Wind classification for the wind speed measured at IJmuiden and the classification boundary for the local conditions.

Wind Class	Wind Velocity (m/s)	Wind velocity corrected (m/s)
1	8	≤ 7.18
2	9-11	7.18 - 8.78
3	12	8.78 - 10.38
4	≥ 13	≥ 10.38

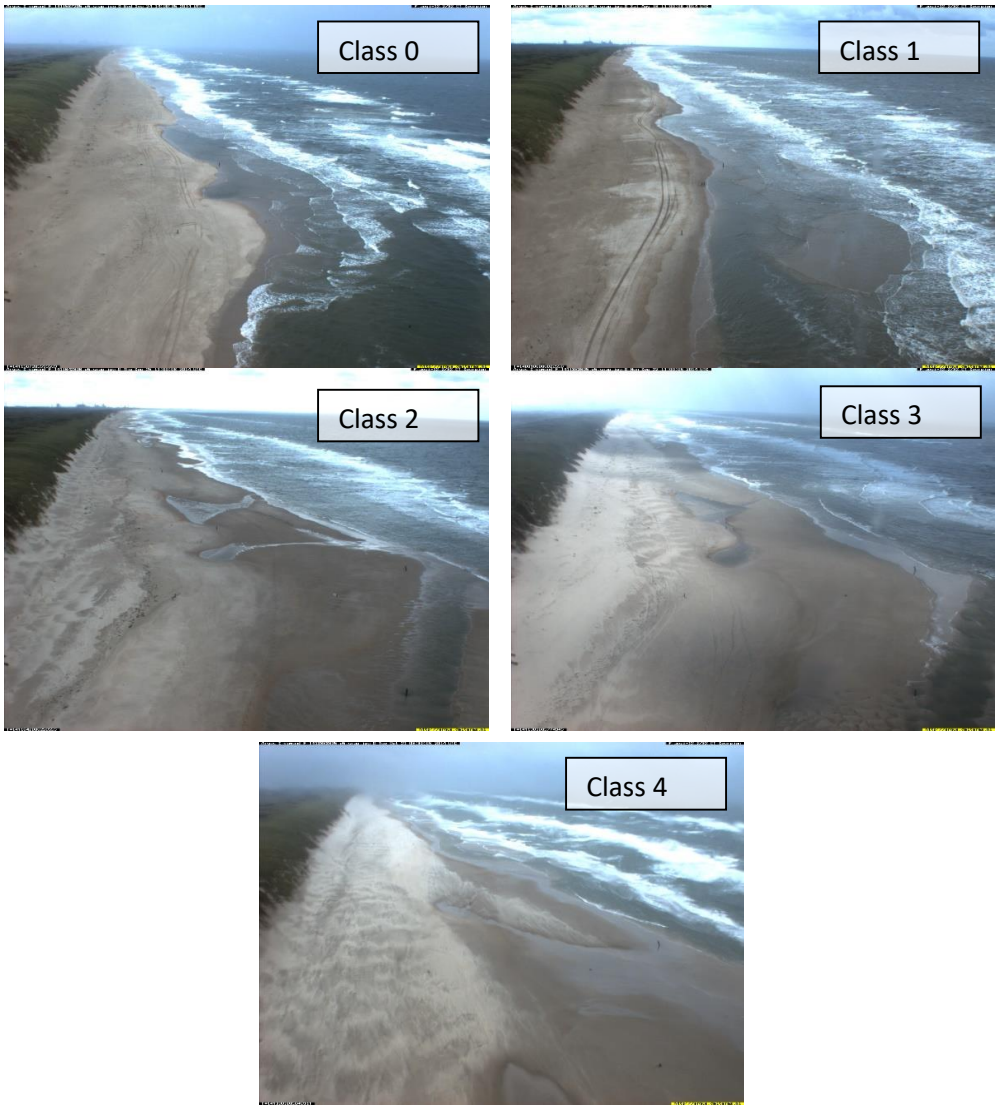

Figure 3.3 Examples of transport activity categories taken by camera 5 (south facing).
class 0 is taken at 24/09/2014 wind direction is 295° and wind speed 8.9 m/s.
Class 1: is taken at 16/08/2014 wind direction 262° wind speed 11.4 m/s.
Class 2: is taken at 25/09/2014 wind direction 251° wind speed 10.7 m/s.
Class 4: is taken at 22/09/2014 wind direction 355° wind speed 12,0 m/s.
Class 5: is taken at 21/12/2014 wind direction 240° wind speed 11.7 m/s.

3.4 Aeolian transport model Aeolus

The model that will be used is developed by Utrecht Coastal Group and can be separated into 3 sections: 1) Groundwater Model; 2) Surface Moisture Model; 3) Aeolian Transport Model. With the right input data, it is possible to run each section as a separate model, and all three sections combined are referred to as the Aeolus model. The Aeolus model produces two outcomes. The first outcome is the potential sediment transport rate, based solely on wind speed; and the actual sediment transport rate, which includes the fetch effect and the effects of soil moisture. The potential sediment transport outcome is referred to as 'wind-only' because it represents the outcome of old aeolian transport models. The beach profile used by the Aeolus model is shown in Figure 3.4.

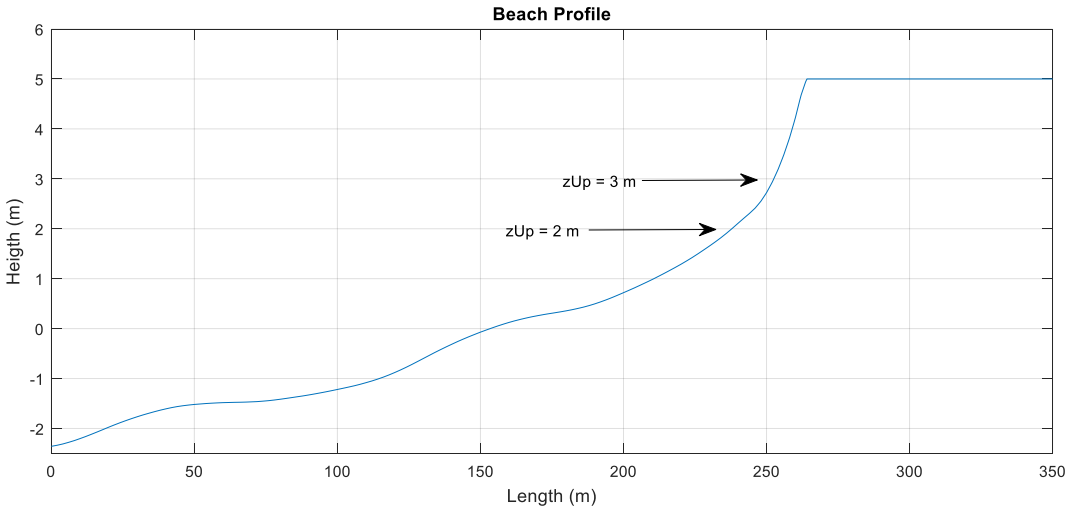

Figure 3.4, the beach profile used by Aeolus. The upwind boundary changes per time step and is therefore not indicated. The downwind boundary is indicated with the arrows and depends on the value of zUp which is either zUp= 2 m or zUp= 3 m.

Groundwater and Surface Moisture model

The groundwater model can run separately from the fetch and aeolian transport functions. In the article of Brakenhoff et al. 2018, a more extensive description of the groundwater model and the implementation of the formulas can be found. The groundwater model uses the following input data: wave height, wave period and bed profile. Furthermore, it requires some parameters which are listed in table 3.2. Through various steps and equations, the ground water level is calculated.

The model starts by determining the and set-up based on the input data, using the parameterization of Stockdon et al. (2006). In addition, the model calculates the location of the shoreline for each time step (t) determined by the user, which was set here to 10 minutes. The shoreline variation (η'_{sh} (x_s,t)) is based on the tidal elevation (ζ_0), in combination with the breaking induced set up (ζ'_{sh}):

8. $$\eta'_{sh}\,(x_{sh},t) = \zeta_0(t) + \zeta'_{sh}\,(t)$$

After indicating the seaward boundary, the run-up infiltration can be calculated. The next step is determining the ground water level. The spatial and temporal water table fluctuations are calculated by

using the non-linear Boussinesq equation, which is extended to include run-up infiltration (U_I) (Brakenhof et al., 2018):

$$9. \quad \frac{\partial \eta\prime(x,t)}{\partial t} = \frac{K}{n_e}\frac{\partial}{\partial x}\left\{[D + \eta'(x,t)]\frac{\partial \eta'(x,t)}{\partial x}\right\} + \frac{U_i}{n_e}$$

Where x is the cross-shore location, K is the hydraulic conductivity of the sand, n_e is the (non-dimensional) specific yield and D is the aquifer thickness. The values of the variables are listed in table XXX. The groundwater level is a time-varying cross-shore profile returned on a spatiotemporal grid with a grid size of 0.5m and a time step of 2 s. The model assumes that the water table is hydrostatic.

With the use of an adapted water retention curve formulated by Van Genuchten (1980), the content is calculated with:

$$10. \quad w'_s(x,t) = w_{res} + \frac{w_{sat} - w_{res}}{[1+(\alpha h(x,t))^n]^{1-1/n}}$$

Whereby w_{res} is the residual gravimetric water content, w_{sat} is the saturated gravimetric water content, h is the depth of the water table, α and n are parameters depending on the shape of the moisture profile. The values of the variables are listed in table 3.2. The outcome, w'_s, is the moisture surface content stored in a spatial and temporal grid for the full beach profile from January 1, 2013 to December 31, 2014. The moisture content values are rounded to 0,5%. This is done because of the nature of the calculation of the critical fetch. The critical fetch is determined for each section with equal moisture content. If the content varies on 0.1%, then in many cases the length of equal moisture content is 1 grid cell, which result in a critical fetch length of 0. Therefore, the moisture content values are rounded.

Table 3.2 the parameters values used for the groundwater model.

General Groundwater and Surface Moisture Model Settings	
Start data	1-1-2013; 00:00
End data	31-12-2014; 24:00
Time step	10 min
Groundwater Model Settings	
Time step ground water level	2 sec
Grid size	0.5 m
aquifer depth	7 m
Hydraulic conductivity	3.5 e -04 m/s
effective porosity	0.3
infiltration coefficient	0.2164
minimum water table depth in runup-infiltration	0.2m
Soil-Water-Retention Curve Settings	
$\mathbf{w_{sat}}$	20.51
$\mathbf{w_{res}}$	2.92
α	5.59 m^{-1}
n	3.69

Table 3.3 The values for the aeolian transport model Aeolus. The zUp value of 2 m and 3 m was used. The wind speed minimum for corrected and uncorrected wind condition is 6.39 m/s and 8 m/s respectively

Aeolian Transport Model Settings	
aHsu	4
D50	240 e -6 m
Surface Moisture Maximum	10%
zUp	2 or 3 m
Wind Speed Minimum	8 m/s or 6.39 m/s
Wind Direction boundary	-90° - 90°

.

Aeolian Transport Function

The Aeolian transport model is the final step of the Aeolus Model and combines the previously computed data and produces the Aeolian transport per time 10-minute intervals. The parameters and criterion which are used are listed in table 3.3.

Within this section of the script, the wind data is adjusted to the local wind conditions. Both the wind speed as the wind direction at the beach of Egmond aan Zee differ from the measurement location of IJmuiden. The regional wind speed is corrected and results in a lower local wind speed. The adjustments for the wind are modeled by multiplying the regional wind speed with the correction factor. The correction factor differs per wind speed (figure 3.5) The computed wind speed is applicable for the entire beach profile (Fig. 3.6 and 3.7). The wind direction is separated into the wind direction at the upwind boundary and downwind boundary. At the upwind boundary the local wind direction is equal to the regional wind direction (Figure 3.2 and 3.5). At the downwind boundary a correction factor is added, because the wind direction is pushed into a more alongshore direction by the dune row. The value of the correction factor depends on the wind direction (figure 3.5). Figure 3.7 shows the wind direction at the downwind boundary. The model calculates two aeolian sediment transport rates, using two wind data sets: one for the beach, one near the dunes (Fig. 3.6 and 3.7). The correction factor for the wind conditions is determined by field research conducted in 2017. The correction factor is implemented with the use of interpolation. To distinguish the importance of correcting the wind condition, the model, both the 'wind-only' and the Aeolus part of the model, are run with the corrected wind data and the data measured at IJmuiden.

The corrected wind conditions are used to calculate the potential transport rate ('wind-only' model) and Aeolus transport rate (Aeolus model). The wind direction is reformulated to shorenormal whereby the northward boundary is + 90° and southward boundary is - 90°. After the conversion of the wind conditions, the model continues determining the width of the beach for each time step.

The width is calculated by the based on the surface moisture content and a fixed back beach boundary. The upwind boundary is the first grid cell whereby the moisture content is equal to 10 %. With a higher moisture content, the surface is too wet for aeolian transport. The downwind boundary is fixed and determined by the parameter zUp (m) which indicates the height of the dune foot. Aeolus was run twice, once with a zUp = 2 m and the second time with zUp = 3 m (see Figure 3.4). These values represent the minimum and maximum value for zUp. The value of zUp was varied to analyse the sensitivity and importance of this parameter.

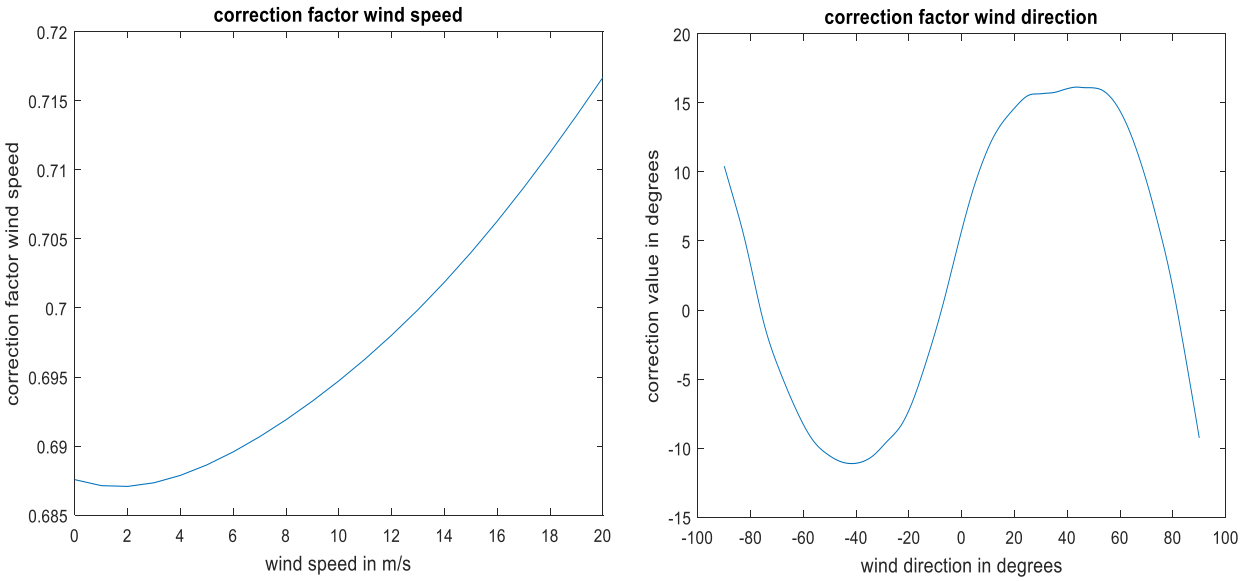

Figure 3.5: left figure shows the correction factor for the regional wind speed. The regional wind speed is multiplied with the corresponding correction factor. Right figure the correction factor for the wind direction. The correction factor is added to the regional wind direction.

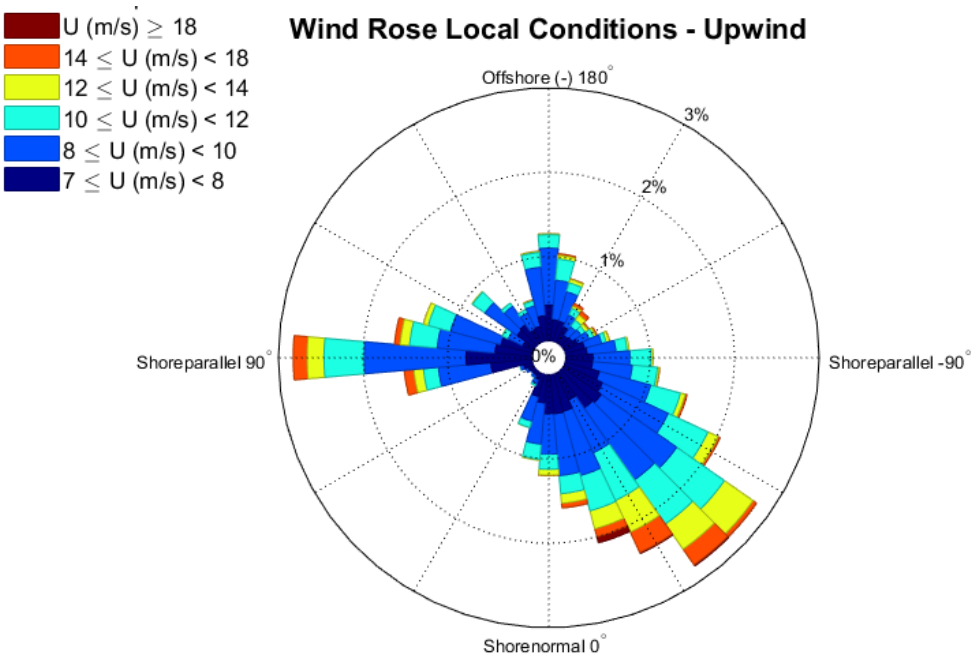

Figure 3.6 The wind speed and direction after the measured wind data is corrected for the local conditions at the upwind boundary of the beach.

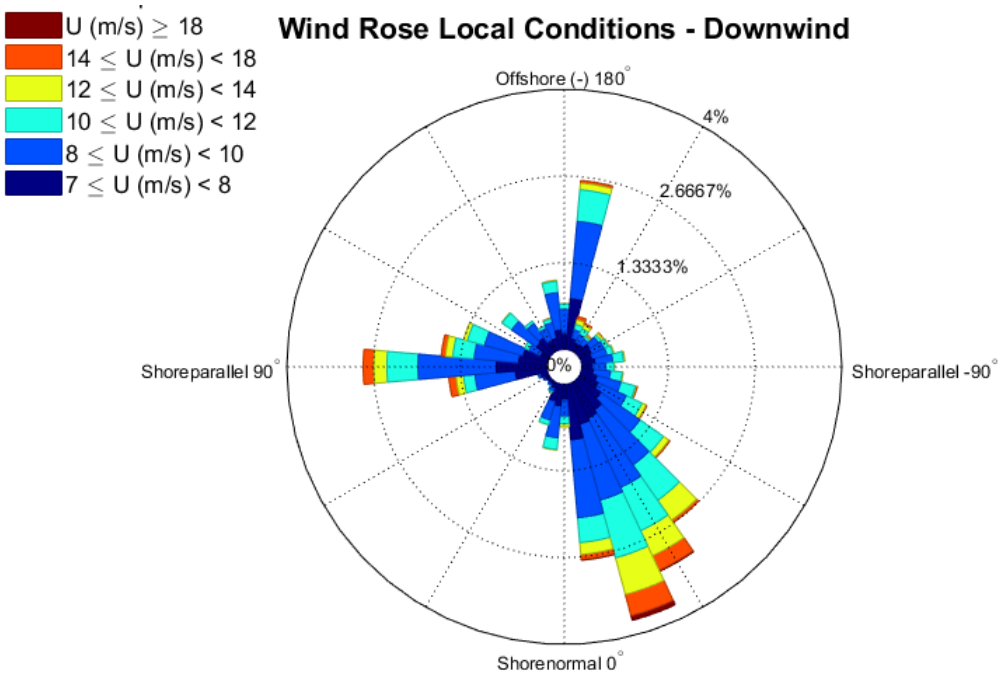

Figure 3.7 The wind speed and direction after the measured wind data is corrected for the local conditions at the downwind boundary of the beach.

The model produces a transport rate of zero (q_n = 0) if the wind direction exceeds (-) 90° and if the wind speed is below the entrainment threshold, which can be determined by the user, but was set here to 8 m/s. After this devision, the potential transport rate is calculated based on only the wind velocity with the use of the Hsu equation (Eq. 12).

$$11.\ qHsu = 1.17 \cdot 10^{-5} \cdot U^3$$

To calculate the Aeolus transport rate, a division is made based on the moisture content of the beach. If the whole beach has a moisture content above 10%, because of inundation or an extremely narrow beach, then no entrainment can occur and no transport occurs. If a part of the beach has a moisture content below 10%, the model calculates the critical fetch.

The model calculates the critical fetch for each time step and each, resulting in a spatial and temporal varying critical fetch value. The critical fetch is calculated by a separate function, which is incorporated within the Aeolian transport model. The advantages of this approach are that the overarching function already filters the data based on the selection criterion. Resulting in a moisture content which is always between 0 – 10%, rounded at 0.5, and a wind speed which is always higher than the threshold of 8 m/s. The moisture content determines the value of the correction factor alpha (α) (Fig 3.8). The higher the moisture content, the higher the correction factor and the higher the critical fetch becomes. The correction factor increases linearly from 1 for a moisture content value lower than 4% to a correction

factor of 1.75 for a moisture content value of 10%. After determining the correction factor, the critical fetch is derived via Delgado-Fernandez equation (2011):

$$12.\ F_c = \alpha \cdot (4.38 \cdot U - 8.23)$$

With F_c and wind speed in m/s. This script generates a spatial grid containing the critical fetch values for each time step.

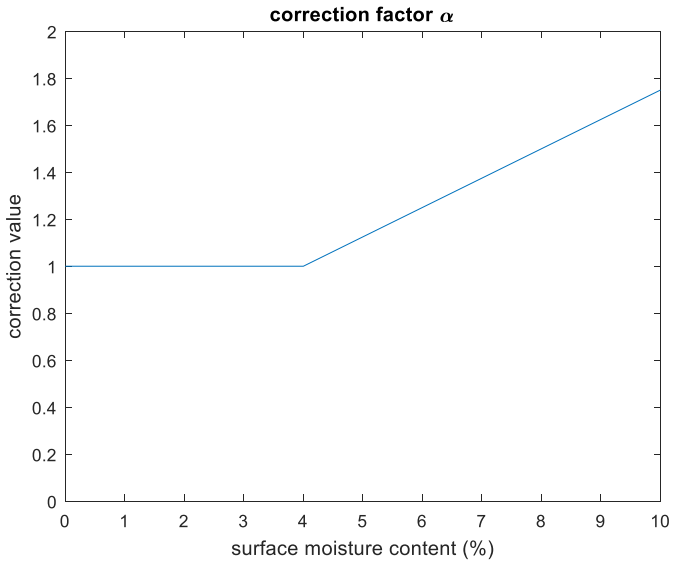

Figure 3.8 shows the value of the correction factor α. The higher the surface moisture content, the higher the correction value and the longer the critical fetch is.

Next is calculating the maximum available fetch for each section. The fetch of the first upwind cell that does not belong to the selected section, in other words, the first cell upwind with a different moisture content, is set to zero. The end of the fetch is the last grid cell of each group of equal moisture content. F cannot exceed Fc, because that would make the sinus term in equation 13 negative. The critical fetch and available fetch are compared to determine the which equation must be used. If F = Fc, then there is unlimited transport and the Aeolus transport is equal to the potential transport rate. If F < Fc, then the transport event is limited and the equation proposed by Delgado-Fernandez (2010) is warranted. This equation is modified to calculate the aeolian transport per location along the cross-shore profile:

$$13.\ qAeolus = q(x-1) + qHsu \cdot sin\left(\frac{\pi}{2} \cdot \frac{F}{F_c}\right)$$

With q, q_{Actual} and $q_{Potential}$ are in kg/m/s. Note that for each time step the value of the actual transport rate could never exceed the value potential transport rate. It can be exactly the same if the transport event is unlimited or lower if it is a limited event.

To sum up for calculating the aeolian transport rate, Aeolus takes into account the beach inundation, the local wind conditions and surface moisture content based upon the tidal elevation, wave-runup, wave infiltration and the groundwater table. The Delgado-Fernandez (2011) includes similar features, however The Aeolus model and Delgado-Fernandez model differ on several points. First, the moisture content in the Aeolus model varies per grid cell, whilst Delgado-Fernandez uses an average value for the entire beach. In addition, Delgado-Fernandez determines the averaged value of the moisture content by measurements, while Aeolus calculates the spatial and temporal surface moisture content. Second, the Delgado-Fernandez model determines an average value is for the fetch and critical fetch. The Aeolus model calculates multiple values for the fetch and critical fetch according to the moisture content. Final difference is the aeolian transport rate. The Delgado-Fernandez model calculates one transport rate, based on the averages of the fetch, critical fetch and moisture content. The Aeolus model produces an aeolian transport rate for each location and all rates combined result in the aeolian transport rate per time step. Overall the difference between Delgado-Fernandez Model and Aeolus is the varying values along the bed profile.

Comparison of Argus and Aeolus outcome

The purpose of this research is to validate the timing of the model. To achieve this, it is necessary to compare these model results with that of the Argus results. The model computed a transport rate for every 10 min for the full computational time, while the Argus images are chosen based on the wind velocity and visibility. Therefore, only the model results that correspond to the date and time of the Argus images are selected. The wind data used by Aeolus is more accurate. Therefore the Argus images are filtered once more for the wind direction and wind velocity. In total there are 2,275 events for the no wind correction scenarios. Due to the correction some events did not meet the threshold criteria and therefore for the scenario with wind correction, there are 2,267 events.

4. Results

The results of the two methods, the Argus imagery and Aeolus Model, are presented below. Between the scenarios with regional and local wind conditions, the numbers of events differ from each other because of the different threshold values of 8 m/s and 7.18 m/s, respectively. In total 8 events did meet the regional threshold and failed the local threshold.

4.1 Results Argus Imagery

Argus result below the model threshold

With the use of 2 images per event, a total of 16,580 images were analysed and classified, which resulted in a total of 3,886 transport events. The Argus images were selected with the generic regional wind speed (wind speed rounded to 1 m/s), while the model uses a very precise data base and had an additional threshold for the wind direction. Some events that were classified with Argus were therefore below the thresholds used by the model. According to the model, if the wind conditions are below the threshold there is no aeolian transport. In total 1611 classified Argus events were below the wind condition thresholds. Table 4.1 shows the transport classification of those 1611 events. If the wind conditions were below the threshold, it follows that no transport occurs. However, Table 4.1 shows that in total 656 events were assigned with a transport class of 1 or higher. Thus, based on the Argus imagery, aeolian transport does occur for wind conditions below the thresholds. It is important to note that for 65 events, the images were classified with the highest transport intensity. This indicates that either or both of the thresholds are not representing the actual thresholds.

To identify in which conditions aeolian transport occurred, a subdivision was made. In Table 4.1 there are two categories:

1) wind speed, and possibly wind direction, did not meet the threshold
2) the wind direction did not meet the threshold.

The results in table 4.1 indicate that for both categories transport events occur and it can therefore be stated that both critical values are not representing the actual threshold for aeolian transport events. The second category contains the majority of the transport event and therefore the wind direction is the threshold with the largest mismatch between natural critical values and the manually implemented threshold.

Figure 4.1 shows the wind direction and speed for all of the 1611 events. Of interest are the wind directions for wind events with a velocity of 8 m/s or higher. In nearly all cases the wind direction just exceeds (-)90°. Thus the threshold of 90° - -90° for the wind direction is too strict because just slightly above 90° there are aeolian transport events. In summary, both thresholds do not represent the actual aeolian transport thresholds, because aeolian transport does occur outside the manually implemented parameter range.

Table 4.1 The number of events that are below the wind condition threshold, and their assigned transport classes. A distinction was made based on the wind velocity. Category 1 indicates that the wind speed, and possibly wind direction, did not meet the threshold. Category 2 indicates that the wind direction did not meet the threshold.

	transport class						
wind speed	0	1	2	3	4	total	total transport events
category 1: <8 m/s	580	82	43	39	15	759	179
category 2: >8 m/s	375	181	157	89	50	852	477
total	955	263	200	128	65	1611	656

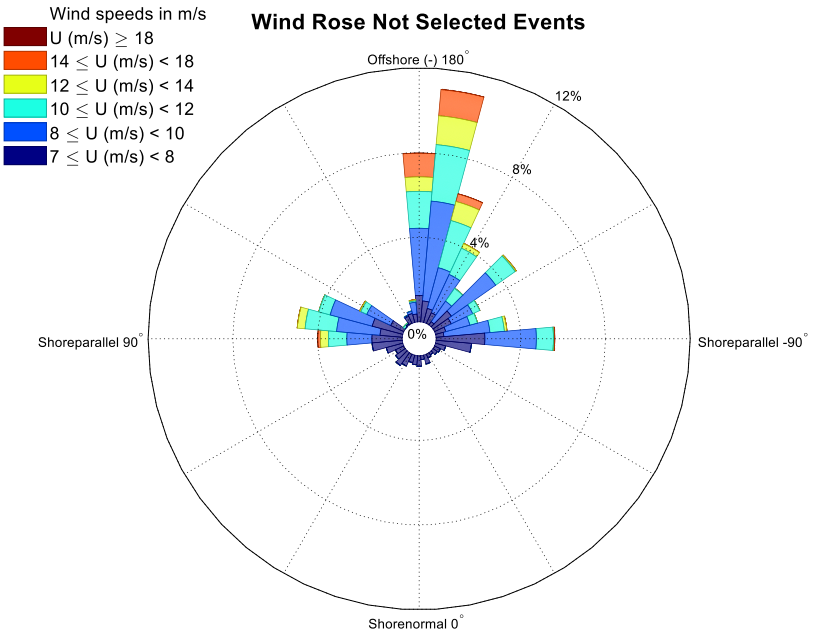

Figure 4.1 shows the wind speed and direction for the events that were discarded because the wind conditions did not meet the criteria determined in the model. North is 97°.

Argus result above the model threshold

In total, the wind conditions did meet the required threshold values in 2,275 out of 3,886 cases. More specifically, there are 2,275 events for the regional wind conditions and 2,267 events for the local wind conditions (table 4.2 and 4.3). The higher the wind class, the larger the potential aeolian transport rate is. However, as the literature and previous experiments show, this high potential does not necessarily translate into actual high transport events (Delgado-Fernandez & Davidson-Arnott, 2011b). For moments with limiting conditions, for example short fetch length or high moisture content, the transport activity can be reduced or even inhibited. The red colour in table 4.2 and 4.3 indicates inhibited events with no aeolian transport and the blue colour indicates limited events. The unlimited conditions in which the transport intensity matches with the wind class are indicated in green. Low wind class numbers (1 and 2) combined with a high transport class (3 or 4) can only occur when the available fetch exceeds the critical fetch drastically. As the beach of Egmond is a narrow beach, this is most likely to occur during oblique wind directions.

To evaluate the results of the Argus model, it is necessary to analyse the events that are unlimited, limited and inhibited separately. In unlimited situations, there are no fetch or supply limiting factors influencing the transport rate. For limited transport events, supply and fetch limiting factors reduce the transport rate. Inhibited transport event indicate that the influence of the limiting factors is of such a large extent that there is no aeolian transport. The classification per type of event is listed for the regional condition in table 4.2 and for the local condition in table 4.3. For the regional wind condition, there are 1,739 events in total (the sum of the limited and inhibited events) that are affected by fetch and supply limiting factors. For 1205 events, the influence of limiting factors caused inhibition of aeolian transport. Only 536 out of 2,275 events are not affected by limiting factors. For the local wind condition, there are 1752 events affected by limiting factors, of which 1,153 cases of total inhibition. Only the remaining 515 events were unaffected by limiting factors.

Between the two scenarios: regional and local wind conditions, there are some differences. For example, for the low wind classes (1 and 2) the number of unlimited transport events is lower in the local wind scenario. Furthermore, for the high wind classes, the number of limited transport events for the local wind conditions has increased. This difference is partly the result of the difference in total events, which was due to the regional and local wind thresholds. Secondly, in some scenarios, an event can be classified in a different wind class after the correction, see table 3.1.

Table 4.2 indicates the number of events for a certain wind- and transport class. This table summarizes the result for the regional wind condition. The red colour represents inhibited events, the blue colour indicates limited events and the green colour indicates unlimited events.

	Argus regional wind condition								
	transport class								
	0	1	2	3	4	Total	total unlimited	total limited	Total inhibited
wind class 1	278	53	25	21	12	389	111	0	278
wind class 2	474	122	62	87	72	817	221	122	474
wind class 3	216	80	61	41	82	480	123	141	216
wind class 4	237	96	122	53	81	589	81	271	237
Total	1205	351	270	202	247	Total transport events:			2275
total unlimited	0	53	87	149	247	Total unlimited transport events:			536
total limited	0	298	183	53	0	Total limited transport events:			534
Total inhibited	1205	0	0	0	0	Total inhibited transport events:			1205

Table 4.3 indicates the number of events for a certain wind- and transport class. This table summarizes the result for the local wind condition. The red colour represents inhibited events, the blue colour indicates limited events and the green colour indicates unlimited events.

	Argus local wind condition								
	transport class								
	0	1	2	3	4	Total	total unlimited	total limited	Total inhibited
wind class 1	292	40	12	20	6	370	78	0	292
wind class 2	472	133	59	66	41	771	166	133	472
wind class 3	195	110	81	65	95	546	160	191	195
wind class 4	194	81	124	70	111	580	111	275	194
Total	1153	364	276	221	253	Total transport events:			2267
total unlimited	0	40	71	151	253	Total unlimited transport events:			515
total limited	0	324	205	70	0	Total limited transport events:			599
Total inhibited	1153	0	0	0	0	Total inhibited transport events:			1153

4.2 Result Aeolian Transport Model

'Wind only' Model results

The Aeolus model produces two results: the potential transport rate ($q_{potential}$) calculated as a 'wind-only' model and a transport rate (q_{aeolus}) based on the supply and fetch limitation implemented in the Aeolus model. The results of the model are filtered based on the date and time to find the corresponding Argus classification of the transport intensity. The model outcome is categorized based on the wind classification (table 3.1) and the transport intensity classification (Argus results). The same colour scheme as in table 4.2 and 4.3 are used for limited, unlimited and inhibited transport events. The potential transport rate is given in table 4.4a and 4.3b in kg/m. The aeolian transport rate in the first (red) column of table 4.4a and 4.3b should be zero, because no aeolian transport was observed. However, the 'wind only' model did calculate a transport rate, which is one the reasons for the large overestimation of the actual transport rate.

Table 4.4a and b indicates which classes, according to the 'wind-only' model, are the main contributors to the overprediction. The transport rate increases for higher wind classes. For the regional wind conditions, the values are significantly higher than for the local wind conditions. The difference in transport rate is a direct result of the lowering of the wind speed for local conditions. The calculation of the transport rate $q_{potential}$ includes the wind speed raised to the power three, which explains the large difference between table 4.4a and 4.4b.

Aeolus Model results

The Aeolus results (q_{aeolus}) are compared to the potential results ($q_{potential}$). The differences between the actual and potential transport rates are expressed in percentages and are listed in table 4.4 c, d, e, and f. For zUp = 3 m, all the unlimited transport rates, apart from one are equal to the potential transport rate: $q_{aeolus} = q_{potential}$. This indicates that for all the unlimited transport events the maximum available fetch exceeded the critical fetch and that at the dune-beach interface the transport rate is equal to the potential transport. For the unlimited transport events for zUp = 2 m, there are multiple results showing a difference between q_{aeolus} and $q_{potential}$. If the zUp parameter equals two meters, the width of the beach is reduced, see Figure 3.4. The difference between the transport rates of Aeolus and the potential indicates that according to Aeolus, the maximum transport rate at the beach-dune interface was reached. This in turn indicates that the maximum available fetch was smaller than the critical fetch. Thus, there are many events for which the critical fetch is not reached with zUp = 2m, but it is reached with zUp = 3m, due to a wider beach.

For the limited transport events, the Aeolus transport rate differs more significantly from the potential transport rate. For the limited transport events each category has a different percentage, however in table 4.4 c, d, e and f the same trend is visible. For both scenarios with zUp = 3 m, the results show a small difference in transport rate compared to the potential rate. The difference is larger when zUp = 2 m and reaches a maximum when it is combined with the regional wind condition. Another trend that is visible in table 4.4 is that the difference between q_{aeolus} and $q_{potential}$ increases towards the bottom left blue corner, implying that the limiting factors become more relevant for a lower transport rate. These conditions indicate that the actual transport rate is strongly reduced by limiting factors, because a wind class of 4 has a very high transport potential. To summarize, two trends are visible for limited transport events: the first is that the transport rate is affected by zUp parameter, and the second is that the limiting factors become more relevant towards the high wind and low transport classes.

For the inhibited transport events, the difference increases with a higher wind class. The higher the percentage, the larger the difference and the closer the model is to a zero transport rate as observed. For wind class 1 and zUp = 3 m there is no difference between q_{aeolus} and $q_{potential}$. For zUp = 2 m there is a small difference. Once more this implies that for a wider beach (zUp = 3 m) the maximum available fetch is equal or exceed the critical fetch. For a narrower beach (zUp = 2 m) the maximum available fetch is smaller than the critical fetch. According to the observation there is no transport. Thus, the outcome of Aeolus should have been zero. Instead, the trend can be observed that the difference between q_{aeolus} and $q_{potential}$ increases for a higher wind class. This implies that the limiting factors are more effective in reducing the transport rate for a high wind class as was the case for the limited transport events. To conclude, the zUp parameter influences all three types of events: inhibited, limited and unlimited. Furthermore, for the limited and inhibited events, the incorporation of the fetch and supply limiting factors are most relevant for high wind classes and low transport class. However, for inhibited transport events, the aeolian transport rate is only reduced, however, according to the observations the transport rate should have been zero.

Table 4.4 a and b indicate the total aeolian transport rate for a certain wind- and transport class. Transport rate is in kg/m. Tables 4.4 c, d, e, and f indicate the difference in transport rate (in percentage) between the 'wind-only' model and Aeolus for regional wind conditions versus local wind conditions and for the dune foot located at 2 m (zUp =2 m) versus the dune foot located at 3 m (zUp = 3 m). The red colour in each table represents inhibited events, the blue colour indicates limited events and the green colour indicates unlimited events.

A Potential transport rate - regional wind

wind class	transport class 0	1	2	3	4
1	640.6	89.4	25.7	46.2	13.5
2	1632.4	482.1	210.7	240.9	154.2
3	1166.1	663.8	491.3	389.3	585.0
4	2654.0	987.7	2156.3	836.5	1616.3

B Potential transport rate -local wind

wind class	transport class 0	1	2	3	4
1	1193.4	229.8	109.5	90.7	52.2
2	3214.4	834.8	434.7	608.8	506.2
3	2512.6	931.5	733.3	501.7	961.8
4	6607.7	2326.3	3749.5	1163.5	2115.1

C q_{Aeolus} regional wind zUp = 3 m

wind class	transport class 0	1	2	3	4
1	0.0	0.0	0.0	0.0	0.0
2	0.1	0.0	0.0	0.0	0.0
3	1.1	0.4	0.0	0.0	0.0
4	14.9	2.0	3.0	0.8	0.0

D q_{Aeolus} local wind zUp = 3 m

wind class	transport class 0	1	2	3	4
1	0	0	0	0	0
2	0.3	0	0	0	0
3	3.1	0.2	1.2	0.1	0
4	27.0	12.1	6.5	3.1	0.8

E q_{Aeolus} regional wind zUp = 2 m

wind class	transport class 0	1	2	3	4
1	2.0	0.0	0.0	0.0	0.0
2	6.7	0.8	0.6	0.5	1.1
3	18.4	10.2	6.0	0.4	0.2
4	43.0	26.0	22.0	4.8	4.1

F q_{Aeolus} local wind zUp = 2 m

wind class	transport class 0	1	2	3	4
1	4.0	0.1	0	0	0
2	12.0	2.3	1.8	0.7	0
3	27.2	13.8	12.3	3.5	2.0
4	58.3	43.9	31.8	13.1	10.1

Aeolus result: transport conditions below threshold

Two important thresholds have already been mentioned several times: the wind speed (8 m/s) and the wind direction (90° - -90°). Table 4.1 shows the Argus classification for events that did not meet the wind speed and/or the wind direction threshold. In 955 out of the total of 1611 events, no aeolian transport was observed and thus in 60.9% of cases the outcome of Aeolus was correct. In the other 40.1%, there was aeolian transport, and in 65 of these events, even a high aeolian transport intensity was observed. Thus in 40.1% of the events Aeolus indicates zero transport, while aeolian transport did actually occur. Overall, the model does not represent the actual transport situation in situations where the wind condition does not meet the threshold for the wind speed and wind direction.

Nonetheless, if the wind speed and wind direction thresholds are met, the observations still indicate that for some events there is no aeolian transport. The inhibition of transport is in this case caused by the supply and fetch-limiting factors. With the incorporation of these factors in Aeolus, the outcome of the model should correspond to the observations. Table 4.4 shows the result of the sum of all inhibited transport events and indicates that the total transport rate is not equal to zero because there is no 100 % difference with the potential transport. Because this table shows the sum of all transport rates for the

transport inhibited regime, it can be that in some events the transport rate is equal to zero. Therefore, table 4.5 shows the number of events that agree with the observations. The correctness of the outcome of the model is assessed by comparing the model outcome with the Argus classification. If the transport class equals zero, then Aeolus should yield q_{aeolus}= 0. If the transport class is larger than zero, Aeolus should output q_{aeolus} > 0. Note that this table only contains those events for which the wind speed and wind direction threshold are met. Therefore, the results relate only to fetch- and supply limitations.

The outcome of the 'wind-only' model is included as well in table 4.5 to indicate if the outcome of Aeolus is an improvement. The 'wind-only' model is solely based on the wind and therefore always generates an aeolian transport rate. As shown in table 4.5, it never agrees with the observations. The Aeolus outcome shows a small improvement compared to the wind-only model. Table 4.5 shows that only for a few events the outcome of Aeolus matches with the Argus observation in terms of the absence of aeolian transport. The transport rate of Aeolus is zero if the moisture content is above 10% or if the beach is very narrow or completely inundated. Table 4.5 indicates that the transport rate is not zero and accounts for approximately (depending on the scenario) 40.1 % of the total aeolian transport rate listed in table 4.6. For zUp = 2 m, more events correspond with the observations and the transport rate is lower. Thus, the width of the beach plays an important role in inhibited transport events. Nonetheless, even with a zUp = 2 m, the outcome of Aeolus for transport class = 0, is only comparable with the Argus observations in 2% of the events and has a total transport rate of 4,616 kg/m.

Both models and nearly all scenarios show a 100% match with the Argus observation for transport class greater than zero. Thus, the timing of the model for observed aeolian transport events is correct (transport class > 0 and q_{aeolus} > 0). The only exception is when the value of zUp is set to 2 m. Then there is a (negligible) 0.2% difference caused by two missing events. For these events the Argus images did show aeolian transport and the Aeolus model produces q_{aeolus}= 0.

Table 4.5 indicates the number of times that the Argus and Aeolus result correspond to the situation of no transport and transport for all of the scenarios. The total transport rate per situation is listed as well as the percentage of the total transport rate.

			Argus	Aeolus			Potential	
			number of events	events matching	transport rate (kg/m)	percentage of total transport	events matching	transport rate (kg/m)
No transport	Regional wind condition	zUp = 2 m	1205	24	8,560	40.7	0	13,528
		zUp = 3 m	1205	1	11,660	44.1		
	Local wind condition	zUp = 2 m	1153	24	4,616	36.5	0	6,093
		zUp = 3 m	1153	1	5,684	39.0		
Transport	Regional wind condition	zUp = 2 m	1070	1068	12,480	59.3	1070	15,349
		zUp = 3 m	1070	1070	14,758	55.9		
	Local wind condition	zUp = 2 m	1114	1112	8,044	63.5	1114	8,988
		zUp = 3 m	1114	1114	8,895	61.0		

Aeolus result: cumulative

The graphs in Figure 4.2 and 4.3 show the cumulative transport rates of q_{aeolus} and $q_{potential}$ for the years 2013 and 2014. The blue line represents the Argus observation. All transport classes are summed and provide a trend line that shows the transport intensity. The trend line shows an increase if the observed transport class was four, and the line is horizontal if no aeolian transport was observed. The magnitude of the increase does not relate to the amount of transport, it only indicates the degree of transport intensity.

The Argus trend line shows a consistent increase, indicating that there are transport events throughout the whole two years. These high transport moments match with the steep increases for the potential and the Aeolus transport rates. This linear increase is visible for both the potential and actual transport rate. In general, it can be stated that the trend line of qAeolus is in agreement with the observed transport events. This indicates as well that the mismatch between transport class = 0 but $q_{aeolus} \neq 0$ and $q_{potential} \neq 0$, does not result in a large overprediction.

All transport lines of both q_{aeolus} and $q_{potential}$ are different. This implies that all the included limiting factors result in a change of the outcome and have to some extent influence on the aeolian transport rate. Furthermore, the $q_{potential}$ rate is always higher than q_{aeolus}, independent of the model settings: regional or local and zUp = 2m or zUp = 3m. This confirms that the fetch and supply limitations are often relevant in reducing the transport rate. The influence of the limiting factors is especially clear during a steep part of the curve where the potential transport rate shows a higher increase than the Aeolus transport rate, resulting in a similar trend, but lower rates for q_{aeolus}. The sum of all the transport rates is listed in table 4.6 and confirms that the transport rate of all scenarios is lower compared to the potential transport rate.

Table 4.6 the cumulative transport rate for all the scenarios for the full-time range (2 years).

Cumulative transport rate			
		Aeolus (kg/m)	**Wind-Only model** (kg/m)
Regional wind condition	zUp = 3 m	26,417	28,877
	zUp = 2 m	21,040	
Local wind condition	zUp = 3 m	14,579	15,082
	zUp = 2 m	12,660	

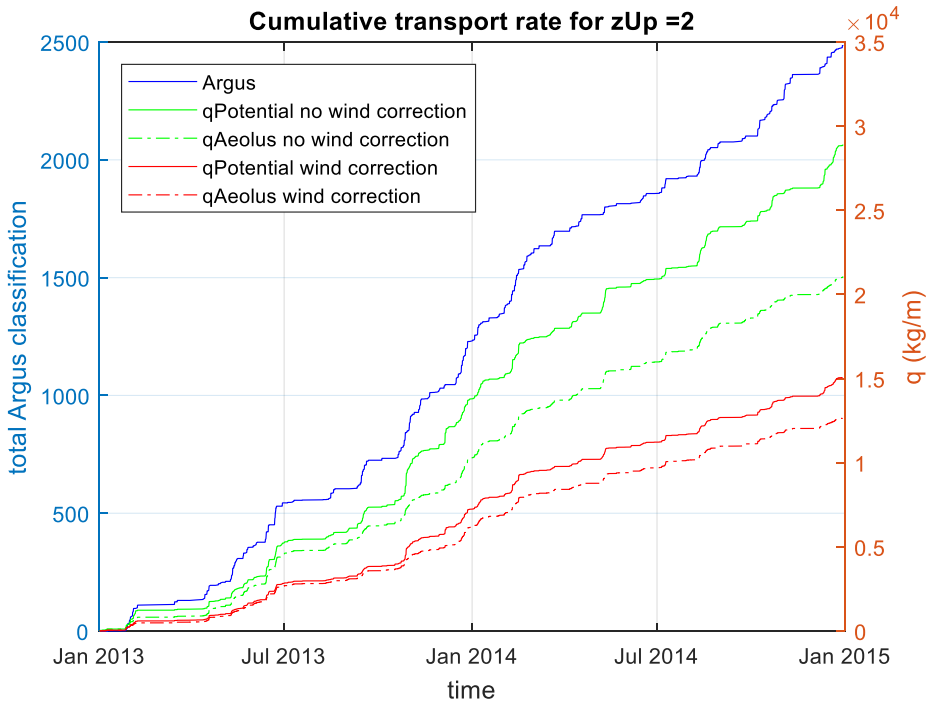

Figure 4.2 shows the cumulative aeolian transport rate for zUp = 2 m. Note that the right-hand y-axis belongs to the transport rate trend lines. The left-hand y-axis belongs to the Argus result. The Argus trend line is the sum of all classes assigned to the analysed images.

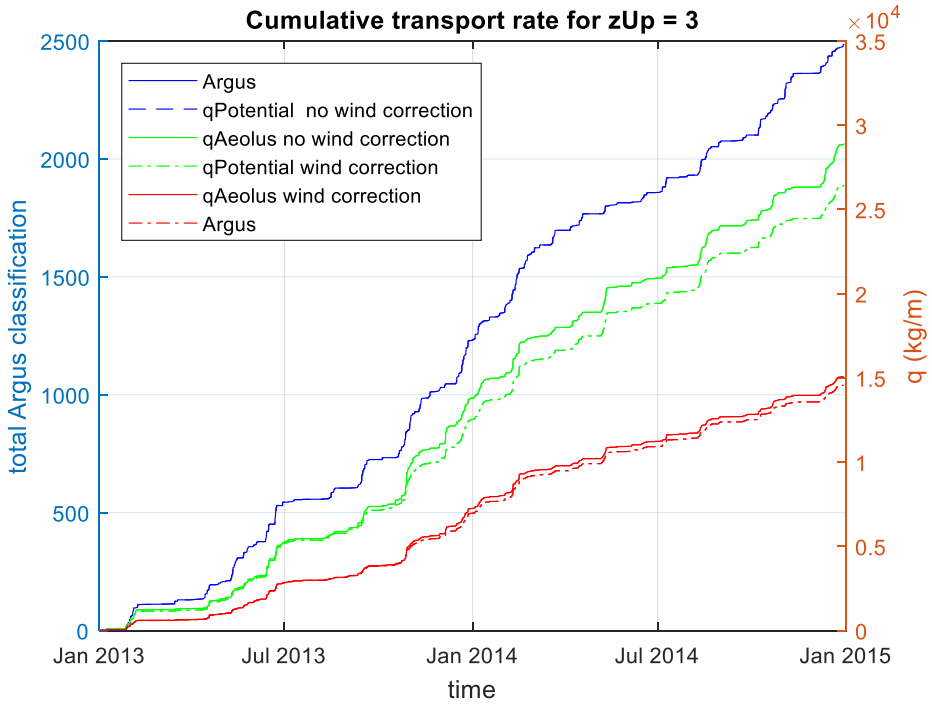

Figure 4.3 shows the cumulative aeolian transport rate for zUp = 3 m. Note that the right-hand y-axis belongs to the transport rate trend lines. The left-hand y-axis belongs to the Argus result. The Argus trend line is the sum of all classes assigned to the analysed images.

5. Discussion

The purpose of this MSc research is to evaluate the validity of a newly designed aeolian sand-transport model, named Aeolus, for its compatibility with natural transport events, with a focus on the timing of the model. The timing of Aeolus consists of three parts: the model produces a zero transport rate when there is no aeolian transport observed, the model generates a transport rate during aeolian transport events and the fetch and supply limitations reduces the transport rate for the correct events.

5.1 Transport conditions

The outcome of the model can be separated into transport and no transport (inhibited) events. Transport events can be subdivided further into limited and unlimited transport events, resulting in a total of three conditions: unlimited aeolian transport events (reaching maximum transport rate), limited transport events (reduced transport rate), and inhibited transport events (no aeolian transport). As explained in the model description, there are supply (i.e. moisture content) and fetch (i.e. variability in shoreline) limiting features incorporated into this model with the aim to improve the outcome for limited and inhibited transport events. The timing of the aeolian model is analysed and validated for all three aeolian transport events.

Unlimited transport events

The 'wind only' model always produces a transport rate when the wind conditions exceed the threshold for wind speed and direction. For unlimited transport events, the outcome of the 'wind-only' model is in full correspondence with the Argus observations. The same correspondence is required for the Aeolus model during unlimited events. The results in table 4.4c and d show that $q_{Potential} = q_{Aeolus}$. This indicates that the timing of Aeolus to produce unlimited transport is unaffected by the limitation factors and that the maximum available fetch exceeds the critical fetch. By only changing the width of the beach, the results in table 4.4e and f show for 12 of the 20 categories $q_{Potential} \neq q_{Aeolus}$. Because only the width of the beach has changed, it is known that the reduction in transport rate is caused by the ratio between the maximum available fetch and the critical fetch. The value of zUp is manually implemented and not an outcome of the model. The values that are used are the minimum and maximum value and not the value related to the beach of Egmond aan Zee. Furthermore, the difference between the potential transport rate and the Aeolus transport rate are relatively small and it can be questioned if the reduction in transport rate will be noticeably affected. Overall the timing of Aeolus in generating the maximum transport rate for unlimited transport events is near to perfect.

Limited transport events

For the limited transport events, the timing of the Aeolus model is in correspondence with the Argus observations, as is also the case for the unlimited transport events. Table 4.4 shows that for a zUp value of 2 m all of the Aeolus transport rates are lower compared to the potential transport rates. The transport of Aeolus is reduced if the maximum available fetch is shorter than the critical fetch. Both the maximum

fetch and the critical fetch are related to supply and fetch limiting factors and for 21 out of the 24 limited transport categories the supply and fetch limitations were relevant. Table 4.4 d and d shows that for three scenarios there is no difference between the potential transport rate and the Aeolus transport rate. For these three categories the critical fetch was exceeded, while the Argus observations showed that there was no maximum transport. In terms of the effect of these 3 categories, in all cases the wind class is relatively low and thus the wind velocity is low as well. It is possible that the classification of limited and unlimited events is inaccurate and that there was indeed unlimited transport. Furthermore, these categories are supposedly only reduced slightly. Thus, most likely the effect of these miss-matches between the model and the Argus observations are small. However, this needs to be verified with actual measurements. Furthermore, the calculations of the critical fetch need to be examined. Nonetheless despite the mismatch of 3, for 21 categories the timing of the model in generating reduced transport rate is done correctly.

Table 4.4 indicates that for the same transport class, for example transport class = 1, the transport rate of higher wind speeds is decreased more than for lower wind classes. This observation can be explained by the critical fetch. A higher wind speed requires a longer critical fetch. As the beach width is narrow, the transport rate during a high wind speed is lower due to the ratio between the fetch and critical fetch. Furthermore, for the categories close to the transition from unlimited to limited, Aeolus shows little difference between q_{Actual} and $q_{Potential}$. In this section the wind class and corresponding transport intensity class indicate that the transport rate is slightly reduced, meaning that the fetch is nearly equal to the critical fetch. whether or not the reductions calculated by Aeolus are correct cannot be stated based on the observation technique. However, the trend of a stronger limitation for a higher wind class and a lower transport class is correct.

inhibited aeolian transport events

On the timing of generating no transport, the new model preforms similar to the wind only model. Both have a (nearly) 100% mismatch with the Argus results. See table 4.5. This indicates that the events are classified with zero transport while the Aeolus model does calculate a transport rate. The transport on the beach is not actually measured but observed with the use of photos. It is most likely that extremely small amounts of aeolian transport are not visually detectible. Therefore, drawing conclusion is to draw conclusions regarding the improvement of the timing of the model compared to actual inhibited transport events.

Table 4.4 and 5.1 shows that the transport rate for Aeolus is reduced greatly compared to the potential transport rate. This reduction, compared to the 'wind-only' model, is the result of the supply and fetch limitations. Even though the outcome has already improved drastically, it can be improved further. Both in terms of the matching events as in terms of the transport rate (Table 4.5). The transport rate calculated for events where no aeolian transport is observed, accounts for 40.1% of the total transport rate of two years. The exact transport rates and the observation method might not be fully reliable for detecting extremely low transport rates. Nonetheless the transport rates are too high. This can either be due to thresholds which are not restrictive enough or a critical fetch which is too small. Therefore, both the thresholds and the calculations for the critical fetch need to be re-evaluated.

In spite of the relatively high transport rate, the model represents the Argus observations. This is confirmed by plotting the cumulative trend line of the Argus classification and the trend line of both of the models, see Figure 4.2 and 4.3. Note that there are two y-axes. Both the models, 'Wind only' and Aeolus, have a similar trend line as Argus. The main difference is the transport rate per event, however all the trends: fast increase (high transport), low increase (low transport) and (nearly) horizontal, are seen for both the models. This trend line confirms that during all sorts of transport events (no, low, medium and high intensity) the model represents the observation.

Under which conditions are the fetch and supply limitation most relevant?
The fetch and supply limitation are irrelevant for unlimited events. This leaves the semi and full limited conditions. The most relevant condition is determined by the largest reduction in transport rate. For that the results are all compared to the potential transport without wind correction. See table 5.1. The largest difference is 77% and is observed in table 5.1c. This is a situation with the highest wind class (> 13 m/s) and no aeolian transport visible. Out of all the categories, this particular category represents the most extreme cases of restriction and are thought to represent storm conditions including; high moisture content, high water table, and, partly or fully inundation of the beach. To verify these conditions, images of the 237 events (based on table 4.2) were analysed once more to list which conditions caused full transport limitation.

The results are shown in table 5.2. In most of the cases there was a combination of conditions visible that prevented aeolian transport. A common example is the combination of rain scatter (meaning that it just had or was soon start to rain) and a high surface moisture content. These two factors are obviously related to each other. The two main factors were: high water levels as a result of storm surges and second, high moisture content which is either due to precipitation or a lack of drying. Thus, the supply- and fetch limiting factors are most relevant under inhibited conditions caused by either high moisture content or storm surges.

5.2 Model implemented features

All the implemented features can be narrowed down into; wind correction, critical fetch and surface moisture content. Furthermore, the influence of the location of the dune foot (zUp) was tested because the exact transition height of the beach into the dunes was not determined and, this parameter might change over time. The beach and dunes are a dynamic system and can change in a single storm event, eroding the dune face. Therefore, it is important to establish the sensitivity of this model for the fetch and supply limiting factors and the zUp parameter.

Table 5.1: The difference of each Aeolus outcome compared to the potential transport rate calculated without wind correction.

A	qActual wind correction zUp = 3 m				
	transport class				
	0	1	2	3	4
1	46.3	61.1	76.5	49.0	74.1
wind 2	49.3	42.3	51.5	60.4	69.5
class 3	54.1	29.0	33.0	22.4	39.2
4	65.8	58.4	44.2	28.7	23.6

B	qActual no wind correction zUp = 3m				
	transport class				
	0	1	2	3	4
1	0	0	0	0	0
wind 2	0.3	0	0	0	0
class 3	3.1	0.2	1.2	0.1	0
4	27.0	12.1	6.5	3.1	0.8

C	qActual wind correction zUp= 2 m				
	transport class				
	0	1	2	3	4
1	47.4	61.1	76.5	49.0	74.1
wind 2	52.6	42.7	51.8	60.6	69.9
class 3	62.1	36.0	37.0	22.7	39.3
4	77.1	68.6	55.2	31.5	26.7

D	qActual no wind correction zUp= 2 m				
	transport class				
	0	1	2	3	4
1	4.0	0.1	0	0	0
wind 2	12.0	2.3	1.8	0.7	0
class 3	27.2	13.8	12.3	3.5	2.0
4	58.3	43.9	31.8	13.1	10.1

Table 5.2:The limiting condition, the number, and percentages of occurrences.

	limiting condition	number	percentage	Total percentage per category
water level	semi high	3	1.3 %	43 %
	back beach inundated	60	25.3 %	
	whole beach inundated	39	16.5 %	
moisture content	semi	28	11.8 %	42 %
	high	72	30.4 %	
weather condition	raining	28	11.8 %	30 %
	rain scatter	44	18.6 %	
other	no visual sign	7	3.0 %	25 %
	doubt	53	22.4 %	
total events		237	100%	

Wind correction limited

Figure 4.2 and 4.3 shows the cumulative evolution of aeolian transport rate of the different scenarios, whereby the largest difference between the 'wind-only' model and Aeolus is due to the wind correction. Both models benefit greatly from the correction from regional wind condition into the local condition and it applies to all situations; unlimited, limited and inhibited transport events. Because the correction applies to both models and all situations, the correction is not a limiting factor. Nonetheless, this correction is a newly added feature of the model and needs to be evaluated.

Using the local wind conditions instead of regional wind conditions improves the model comparability with the natural situation. Naturally, with the use of the local wind conditions, the transport rates become more comparable with the actual transport rates. The difference between the transport rates between the

regional and local wind conditions is extensive. As the literature indicated, the transport rates based solely on the wind speed resulted in a 29 times overprediction, the reduction of this transport rate can therefore be seen as an improvement. Still, in order to be certain that the implementation of the correction factor is an improvement, the transport rate needs to be compared to actual transport measurements.

The field research that resulted in the correction factor for both the wind direction and wind speed, can be done for all beaches and the outcome can be implemented in to an aeolian transport model. However this is inconsistent with the concept of a universally usable computer model. The differences are, however, so significant that a conversion is necessary to represent natural transport conditions and rates.

Surface Moisture Content

Including moisture content factor, reduces the aeolian transport rate for limited and inhibited transport events, see table 4.4. Even though the wind correction leads to the largest reduction of the mismatch, the surface moisture content is also important if we aim to create a model that perfectly reflects reality. The surface moisture content is calculated by combining tidal inundation, wave-runup, storm surges and the depth of the water table. In the previous paragraph, it was discussed that for extreme limited events, the supply and fetch limiting factors were most important. Table 5.2 summarizes what the limiting conditions were. All of the conditions are related to the moisture content and not to the wind conditions. Thus, the wind condition correction results in the largest change, but in the most crucial transport events, the surface moisture content is the most relevant limiting factor.

Sensitivity of the model to the zUp-parameter

The transition from the beach into the dunes is determined by the height of the beach profile. For this research the height was set to 2 m and 3 m, as these are thought to represent the minimal and maximum height of the down-wind boundary. The fetch length is determined for each time step and depends on the varying upwind- and the fixed downwind-boundary. The length of the maximum available fetch is important for the calculation of the transport rate and the influence of limiting factors. Therefore, understanding the sensitivity of this parameter, indicates the degree of influence by the supply and limiting factors.

As shown in table 4.5, the model turns off for 23 more events for a lower zUp value. Compared to the total number of events (1153), the difference made by zUp is minimal. Nonetheless in 22 events the critical fetch was not exceeded for a zUp = 2 m. Furthermore, for the cumulative transport rate over 2 years, the zUp value makes a substantial difference. The difference for the scenario with local wind condition is 1919 kg/m (13 %) between zUp = 2 m and zUp = 3 m, and for the scenario with regional wind condition is 5377 kg/m (20%). This indicates that for a lower value for zUp the supply and fetch limiting factors are more relevant. Limiting factors increase the critical fetch length and with a smaller width due to the zUp value of two meters, the transport rate is lower as a result of equation 13. A 13% and 20% difference is significant and indicates a large influence of supply and limiting factors. Furthermore, due to this sensitivity, the value of zUp needs to be determined very precisely to reduce potentially inaccurate model outcome.

Critical Fetch

The critical fetch is an important factor in determining the aeolian transport rate. The critical fetch is determined based on the wind speed and the surface moisture content. The higher the wind speed and/or moisture content the longer the critical fetch is. Egmond aan Zee is classified as a narrow beach and thus it is expected that for a shore normal wind, the fetch is smaller than the critical fetch. This is confirmed by table 5.3. In only 1,929 out of the 11,907 events, the critical fetch was exceeded and the transport rate was equal to the potential transport rate. The critical fetch is more often exceeded if the wind is oblique to the shore line. If the wind is coming from the south, the critical fetch is not exceeded only 14% of the events while for wind coming from the north this is approximately 50%. This large difference is the result of the shape of the North Sea and the position of the Dutch Coastline. The set-up for a north-western wind is larger compared to a south-western wind, resulting in a narrower beach. Therefore, the fetch is shorter and, in more events, the critical fetch is not exceeded.

However, during the analysis for inhibited conditions, the aeolian transport rate was higher than expected. Inhibited events are caused by the strong influence of the limiting factors. The critical fetch depends on the surface moisture content, but the effect on the lengthening might underestimate the actual effect. Table 5.2 indicate that the moisture content is important for inhibited transport events and the aeolian transport rate depends on the ratio of the fetch and the critical fetch. The length of the critical fetch for inhibited events need to be compared with more data, to determine if the calculations represent actual critical fetch lengths.

Table 5.3 indicates the amount of events whereby the fetch is shorter than the critical fetch and longer than the critical fetch for three types of wind direction: oblique wind coming from the North, oblique winds coming from the South and shore normal wind direction. This is based on the local wind direction and is the Aeolus result for the full 2-year computation.

Overview wind direction and Fm/Fc ratio zUp = 2 m			
Wind direction	Fm < Fc	Fm > Fc	total
direction -90 ° - -20° (oblique North)	14,236	15,362	29,598
direction -20 ° - 20° (cross shore)	9,978	1,929	11,907
direction 20 ° - 90° (oblique South)	806	4,915	5,721
total	25,020	22,206	47,226

Threshold conditions

Within Aeolus there are three defined thresholds: the wind speed of 8 m/s, the wind direction of -90° to 90° and the moisture content of 10%. For the wind condition threshold the values need to be re-evaluated. Table 4.1 indicates that for 656 transport events the model produces a zero-transport rate, contradicting to the observations, as all of these events showed aeolian transport. For 65 of these transport events the Argus images were classified with the highest intensity. As previously discussed, the outcome of the model is correct for transport events whereby the conditions exceed the threshold. Thus, if the values for the wind speed and wind direction are re-evaluated and represent the natural threshold, the model outcome for unlimited and limited transport event can improve the 40.1% mismatch.

The results of table 5.2 indicate that rainfall can inhibit aeolian transport. Currently, this factor is not included in the model. However, table 5.2 indicates that in 72 of the 237 events, rain was one of the causes for inhibited aeolian transport. A possible solution is to use precipitation measurements as data input and use a threshold value to indicate if the rain will reduce or inhibit aeolian transport. Regardless if the rain is incorporated, the results show that rain is an important limiting factor at this study site.

5.3 Method

Argus images were analysed to validate the modelling results. This method is relatively cheap and easy to conduct on a meso-scale. With the use of the images an extensive time-covering data set was established. Many transport events are clear and easily distinguished. Nonetheless, classifying the events is subjective, even with the use of reference images. Partly because the quality and clarity of the images varies hourly and daily due to weather conditions. Furthermore, in order to quantifying the intensity of the transport a contrast between dry moving sand and wet stable sand is required and additionally extremely small amounts of aeolian transport could not or barely be identified. The subjectivity became apparent during the second viewing of the extremely constricted events. When analysing those images a second time, previous classification could be reconsidered. In 53 out of 237 events, it was debatable if there was absolutely no transport or if there might have been some transport. A reclassification would have been from class 0 to class 1; this would favour the outcome of the model as there is so little agreement between the no transport observed and no transport calculated. If these events were indeed incorrectly classified, the interpretation of the model timing would improve.

This validation research was the first to be conducted and to review the timing of the new transport model Aeolus. The results prove that the model preforms correctly during transport events. The model performance during no or extremely low transport rates was, based on this research, not significantly improved compared to the ‘wind only’ model. However, the observations are not accurate enough to rely on and therefore a validation based on these observations can result in a wrongful interpretation.

5.4 Is the timing of Aeolian transport improved by incorporating fetch- and supply limitation?

The timing of aeolian transport, computed by Aeolus, can be separated into three categories: generating a zero-transport rate when no transport is observed, generating a transport rate when transport is observed, and, generating a transport rate that matches the type (limited or unlimited) of transport event.

In the first case, the model generates a zero-transport rate for inhibited transport events. If the results are compared with the 'wind-only' model, the results have improved. Table 4.4 and 4.5 shows a higher number of matching events and a greatly reduced transport rate. However, compared to the observations the outcome of Aeolus can be improved further. This can be done by re-evaluating the threshold conditions and the critical fetch calculations. As table 5.2 indicates the moisture content and the available fetch are the main causes of inhibited transport. Note that the observations are subjective and therefore it is difficult to draw conclusions regarding the improvement of the timing of the model compared to actual inhibited transport events.

Second, the model generates an aeolian transport rate when aeolian transport is observed on the Argus images. This category can be split in two sub-categories based on the wind conditions: below model entrainment threshold and above model entrainment threshold. When the wind conditions meet the criteria, meaning the wind speed was ≥ 8 m/s and the wind direction was between –90° and 90°, the model had a perfect timing. The incorporation of the fetch and supply limitation did not affect this. For wind conditions not obeying the aforementioned criteria, the model generated a zero-transport rate, even though there were high intensity transport events observed. This is not due to a malfunctioning model, but a consequence of inaccurate threshold values. For all the observed transport events, both limited and unlimited events, the model generated a transport rate above zero for 60% of the events. This can be improved by re-evaluating the threshold for both the wind speed and the wind direction.

Last, the supply limitation activates for the correct events. For nearly all limited events, the model activates the fetch and supply limiting factors. This is indicated by the difference between the 'wind-only' model and the Aeolus results, see table 4.4. The higher the wind class and the lower the observed transport class, the stronger the aeolian transport is reduced. These results correspond with the relation between the critical fetch and the wind speed. The difference between Aeolus and the 'wind-only' model follows the same increasing trend, indicating that the limitation factors are activated correctly.

Overall the model performs properly. Figure 4.2 and 4.3 show that the Argus and Aeolus results are comparable. This indicates that the overall the model produces a high transport rate for high transport events and the supply and limiting factors are relevant for the correct events. The timing of the model can be improved further, especially for the inhibited events. This improvement can be realised by re-evaluating the computation of the critical fetch and the threshold conditions. Furthermore, the transport rates need to be compared with actual field measurements.

Conclusion

The purpose of this MSc research was to evaluate the validity of a newly designed aeolian sand-transport model, named Aeolus, for its compatibility with natural transport events, with a focus on the timing of the model. The conclusion will be presented per research question.

Is the timing of aeolian transport events improved by incorporating fetch and supply-limitation?

Yes, compared to the 'wind-only' model, the timing of aeolian transport events has improved by incorporating fetch and supply-limitations. For observed transport events the model has a 60% correspondence. This is mainly the result of the implemented threshold for the wind velocity and wind speed and therefore these values need to be re-evaluated. The outcome is similar to the 'wind-only' model. For the events whereby no aeolian transport was observed, the 'wind-only' model never corresponds and Aeolus shows a 0.1% to 2% correspondence, depending on the location of the down-wind boundary. The main improvement of the newly designed model is the agreement for transport events that are limited. In total there were 24 categories which indicated a reduced transport rate and for 21 categories the outcome of Aeolus indicated a limited transport rate.

Under which conditions are fetch and supply-limitations most relevant?

The fetch and supply-limitations were most relevant for the inhibited transport events. For these events the potential transport rate was very high, while no transport occurs. This is one of the reasons for the large overprediction in aeolian transport rate by 'wind-only' models. The implementation of the fetch and supply-limiting factors caused a large reduction in the aeolian transport rate. Because of the used methods, the exact transport rates are unknown. Nonetheless the observations in combination with literature indicated that the transport rate for events whereby no transport was observed, was relatively high. The transport rate calculated for inhibited transport events, contributed for approximately 40.1% to the total transport rate. The outcome can be improved by re-evaluation of the calculations for the critical fetch.

Which of the fetch or supply-limiting factors is most important on a timescale of years to minimize mismatch between wind-only and actual transport events?

The fetch and supply-limiting factor that is most important is the moisture content. Examination of the cause for inhibited transport indicated that the surface moisture content was the most important limiting factor. The surface moisture content is calculated by combining the tidal inundation, wave-runup, storm surges and the depth of the water table. The use of the local wind condition is not a fetch or supply limiting factor, but this feature is most important for the overall minimizing of the mismatch between 'wind-only' models and actual transport events. Based on the results, an additional threshold for rain conditions is suggested.

References

Anderson, R. S., & Haff, P. K. (1988). Simulation of Eolian Saltation. *Science*. doi:10.1126/science.241.4867.820

Bagnold, R. A. (1941). The Physics of Blown Sand and Desert Dunes. *Nature*. doi:10.1038/148480a0

Bauer, B. O. Sherman, D. J. Nordstrom, K. F. Gares, P. A. (1990). Aeolina transport measurement and prediction across a beach and dune at Castroville, California.

Bauer, B. O., & Davidson-Arnott, R. G. D. (2003). A general framework for modeling sediment supply to coastal dunes including wind angle, beach geometry, and fetch effects. *Geomorphology*, *49*, 89–108.

Bauer, B. O., Davidson-Arnott, R. G. D., Hesp, P. A., Namikas, S. L., Ollerhead, J., & Walker, I. J. (2009). Aeolian sediment transport on a beach: Surface moisture, wind fetch, and mean transport. *Geomorphology*, *105*, 106–116.

Brakenhoff, L. B., Smit, Y., Donker, J. J., & Ruessink, G. (2018). Tide-induced variability in beach surface moisture: observations and modelling. *Earth Surface Processes and Landforms*.

Davidson-Arnott, R. G. D., Yang, Y., Ollerhead, J., Hesp, P. A., & Walker, I. J. (2008). The effects of surface moisture on aeolian sediment transport threshold and mass flux on a beach. *Earth Surface Processes and Landforms*. doi:10.1002/esp.1527

Davidson-Arnott, R. G., MacQuarrie, K., & Aagaard, T. (2005). The effect of wind gusts, moisture content and fetch length on sand transport on a beach. *Geomorphology*. doi:10.1016/j.geomorph.2004.04.008

Delgado-Fernandez, I. (2010). A review of the application of the fetch effect to modelling sand supply to coastal foredunes. *Aeolian Research*, *2*, 61–70.

Delgado-Fernandez, I. (2011). Meso-scale modelling of aeolian sediment input to coastal dunes. *Geomorphology*, *130*, 230–243.

Delgado-Fernandez, I., & Davidson-Arnott, R. (2011a). Meso-scale aeolian sediment input to coastal dunes: The nature of aeolian transport events. *Geomorphology*, *126*, 217–232.

Delgado-Fernandez, I., & Davidson-Arnott, R. (2011b). Meso-scale aeolian sediment input to coastal dunes: The nature of aeolian transport events. *Geomorphology*. doi:10.1016/j.geomorph.2010.11.005

Gillette, D. A., Herbert, G., Stockton, P. H., & Owen, P. R. (1996). Causes of the fetch effect in wind erosion. *Earth Surface Processes and Landforms*. doi:10.1002/(SICI)1096-9837(199607)21:7<641::AID-ESP662>3.0.CO;2-9

Hage, P. M., Ruessink, B. G., & Donker, J. J. A. (2018a). Determining sand strip characteristics using Argus video monitoring. *Aeolian Research*, *33*, 1–11.

Hagre, P.M., Reussink, B. G., & Donker, J. J. A. (2018b). Using Argus Video Monitoring to Determine Limiting Factors of Aeolian Sand Transport on a Narrwo Beach. *Marine Science and Engineering*, doi:10.3390/jmse6040138.

Hsu, S. A. (1974). Computing eolian sand transport from routine weather data. In *Proceedings of the Fourteenth Coastal Engineering Conference*.

Keijsers, J. G. S., Poortinga, A., Riksen, M. J. P. M., & Maroulis, J. (2014). Spatio-temporal variability in accretion and erosion of coastal foredunes in the Netherlands: Regional climate and local topography. *PLoS ONE*. doi:10.1371/journal.pone.0091115

Kroon, A., & Hoekstra, P. (1990). Eolian Sediment Transport on a Natural Beach. *Source: Journal of Coastal Research Journal of Coastal Research*.

Masselink, G.; Hughes, G.; Knight, J. (2014). *Introduction to coastal processes & geomorphology* (Second). New York: Routledge.

NICKLING, W. G. (1988). The initiation of particle movement by wind. *Sedimentology*. doi:10.1111/j.1365-3091.1988.tb01000.x

Nickling, W. G., & Neuman, C. M. K. (2009). Aeolian sediment transport. In *Geomorphology of Desert Environments*. doi:10.1007/978-1-4020-5719-9_17

Nield, J. M., & Wiggs, G. F. S. (2011). The application of terrestrial laser scanning to aeolian saltation cloud measurement and its response to changing surface moisture. *Earth Surface Processes and Landforms*. doi:10.1002/esp.2102

Nield, J. M., Wiggs, G. F. S., & Squirrell, R. S. (2011). Aeolian sand strip mobility and protodune development on a drying beach: Examining surface moisture and surface roughness patterns measured by terrestrial laser scanning. *Earth Surface Processes and Landforms*. doi:10.1002/esp.2071

Nordstrom, K. F., & Jackson, N. L. (1993). The role of wind direction in eolian transport on a narrow sandy beach. *Earth Surface Processes and Landforms*. doi:10.1002/esp.3290180803

Sherman, D. J., & Li, B. (2012). Predicting aeolian sand transport rates: A reevaluation of models. *Aeolian Research*. doi:10.1016/j.aeolia.2011.06.002

Sherman, D. J., Li, B. L., Ellis, J. T., Farrell, E. J., Maia, L. P., & Granja, H. (2013). Recalibrating aeolian sand transport models. *Earth Surface Processes and Landforms*. doi:10.1002/esp.3310

Stout, J. E., & Zobeck, T. M. (1997). Intermittent saltation. *Sedimentology*. doi:10.1046/j.1365-3091.1997.d01-55.x

SVASEK, J. N., & TERWINDT, J. H. J. (1974). Measurements of sand transport by wind on a natural beach. *Sedimentology*. doi:10.1111/j.1365-3091.1974.tb02061.x

Walker, I. J., Davidson-Arnott, R. G. D., Bauer, B. O., Hesp, P. A., Delgado-Fernandez, I., Ollerhead, J., & Smyth, T. A. G. (2017). Scale-dependent perspectives on the geomorphology and evolution of beach-dune systems. *Earth-Science Reviews*, *171*, 220–253.

Wiggs, G. F. S., Baird, A. J., & Atherton, R. J. (2004). The dynamic effects of moisture on the entrainment and transport of sand by wind. *Geomorphology*. doi:10.1016/j.geomorph.2003.09.002